

Exact WKB Analysis and TBA Equations for the Stark Effect

Katsushi Ito¹ and Jingjing Yang²

*Department of Physics,
Tokyo Institute of Technology
Tokyo, 152-8551, Japan*

Abstract

We apply the exact WKB analysis to a couple of one-dimensional Schrödinger-type equations reduced from the Stark effect of hydrogen in a uniform electric field. By introducing Langer's modification, we prove the exactness of the Bohr-Sommerfeld quantization conditions for the Borel-resummed quantum WKB periods at the weak electric field intensities from the Stokes graphs. It is also found these quantization conditions get modified with an additional suppressed contribution when the electric field becomes large. We also present Thermodynamic Bethe Ansatz (TBA) equations governing the quantum periods in the absence of Langer's modification and discuss its wall-crossing and analytic continuation. Numerical calculations are conducted to compare the complex resonant frequencies from our quantization conditions against ones from the Riccati-Padé method, the TBA equations are also confirmed by comparing its expansions with all-orders quantum periods.

¹ito@th.phys.titech.ac.jp

²j.yang@th.phys.titech.ac.jp

Contents

1	Introduction	2
2	Exact WKB analysis and connection formulas	4
2.1	Review of the all-orders WKB expansions	4
2.2	Stokes graphs and connection formulas	6
2.2.1	Borel resummation and Stokes graphs	6
2.2.2	Connection formulas and quantum periods	9
3	Stark Effect and its quantization conditions	13
3.1	Langer's modification and boundary conditions	13
3.2	Quantization conditions	16
3.3	Computation and results	23
4	TBA equations and analytic continuation	29
4.1	Singular potentials and quantum periods	29
4.2	TBA equations for the minimal chamber	31
4.3	Analytic continuation and wall-crossing	36
5	Discussion and conclusion	39

1 Introduction

The Stark effect describing hydrogen under an external electric field [1], is one of the earliest examples considered since the invention of quantum mechanics. The external field leads bound states for hydrogen to resonant states, whose energy becomes complex $E = E_c + i\Gamma/2$. E_c represents the peak of the energy spectra and Γ stands for the width related to the ionization rate. There are many approaches based on perturbation theory to solve this problem [2, 3, 4, 5, 6]. But the perturbative expansions for the Stark effect are asymptotic, so additional numerical methods such as Borel-Padé technique are necessary. There are also WKB-type approaches that rely on the fact that the three-dimensional Schrödinger equation for the Stark effect is separable under parabolic coordinates. Both of the separated equations take the form of the one-dimensional Schrödinger equation with a linear and inverse potential in addition to a centrifugal term. To satisfy the correct boundary condition at origin, Kramers and especially Langer [7] introduce the so-called Kramers-Langer substitution or Langer's modification used in this paper, see [8]. A comprehensive interpretation can be found in [9] in terms of two- \hbar notation in an enlightening perspective. The successive research on the WKB method for the Stark problem is almost based on Langer's modification, such as [10, 11, 12, 13]. These works mainly rely on the period integrals in the classically allowed region, which will be notated as classical WKB periods.

The main purpose of this paper is to study the Stark effect by exact WKB analysis. This can be achieved by the Borel resummation of formal \hbar power series in the framework of resurgence theory [14, 15, 16, 17]. The analytic behavior of the Borel-resummed WKB solution is determined by Stokes graphs, and the relation of WKB solutions for different Stokes regions is described by connection formulas [18, 19, 20]. In quantum mechanical problems, one imposes boundary conditions for the wave functions, these deduce the exact quantization conditions (EQCs) for the eigenvalue problems in terms of quantum period [21, 22, 23, 24]. It is Borel-resummed quantum WKB periods appearing to connect the

solutions with different normalizations. Its discontinuity is captured by the Delabaere-Pham formula (DP formula) [25, 26]. In this paper, we apply the exact WKB analysis to the Stark effect to obtain the exact quantization conditions.

The development of WKB analysis invoked the study of integrable models and is formed into the so-called ODE/IM correspondence [27, 28]. ODE/IM correspondence indicates there is a relationship between the Y functions in integrable models and quantum periods from WKB analysis. Specifically, Y systems derived from the Wronskian relations coincide with equations followed by quantum periods from the DP formula [29]. These studies on the one hand introduced new techniques into integral models, on the other hand, fed back the research on the ODE side. Especially the ODE/IM correspondence introduces TBA equations for quantum periods, which provides a non-perturbative completion for these asymptotically defined quantities in WKB analysis. This correspondence was summarized explicitly for polynomial potentials [29, 30] and also potentials with regular singularity [31]. As one analytically continues the parameters in the potential, TBA equations get modified when wall-crossing of quantum periods happens [32]. We would like to consider these kinds of TBA equations corresponding to the reduced one-dimensional equations for the Stark effect.

This paper is organized as follows. In section 2, we review the fundamentals of exact WKB analysis. Our work starts from section 3, which focuses on the application of exact WKB analysis to the Stark effect. We consider Langer's modification and all-orders quantum corrections and write down the exact quantization conditions (EQCs) from the Stokes graph. It is found the Bohr-Sommerfeld quantization condition for the Borel-resummed periods is already exact for weak field strength but gets an additional term when the electric field becomes strong. Our EQCs are numerically tested against the Riccati-Padé method [33]. Section 4 is devoted to finding integral TBA equations for quantum periods. However, these TBA equations are established for bare effective potentials without Langer's modification, which is different from the prescription adopted in section 3. We discussed the wall-crossing of the TBA equations [32] and also the analytic continuation [34, 35] against

the parameters for the Stark effect. We conclude our results in section 5.

2 Exact WKB analysis and connection formulas

In this section, we give a brief review to mention fundamental aspects and fix the notations of the exact WKB analysis applied later. We intensively consult the work of [18, 19, 20, 23, 24] and the references therein for this section.

2.1 Review of the all-orders WKB expansions

The Stark effect involves a couple of one-dimensional Schrödinger equations as discussed in section 3. Let us first consider the equation for a generic potential $Q(x, \hbar)$

$$\left(-\hbar^2 \frac{d^2}{dx^2} + Q(x, \hbar)\right) \psi(x) = 0, \quad (2.1)$$

where

$$Q(x, \hbar) = Q_0(x) + Q_2(x)\hbar^2 \quad (2.2)$$

consists of one classical potential $Q_0(x)$, and an additional \hbar dependent term $Q_2(x)\hbar^2$, usually called quantum potential. The coordinate x is a complex variable, and we regard the reduced Planck constant \hbar as an expansion parameter, which is also taken to be complex and set to 1 in the end. One starts by setting a WKB ansatz

$$\psi(x) = \exp\left(\frac{1}{\hbar} \int^x P(x, \hbar) dx\right), \quad (2.3)$$

where

$$P(x, \hbar) = \sum_0^{\infty} p_n(x)\hbar^n \quad (2.4)$$

is a formal power series. Substitute the above solution for wave function into (2.1), then we arrive at the Riccati equation

$$\hbar P'(x) = Q_0(x) - P^2(x) + \hbar^2 Q_2(x). \quad (2.5)$$

This equality holds to all orders, matching order by order reduces to the following recursive relations for $p_n(x)$

$$p_n(x) = -\frac{1}{2p_0(x)} \left(\sum_{i=1}^{n-1} p_{n-i}(x)p_i(x) + p'_{n-1}(x) \right), \quad n \geq 3, \quad (2.6)$$

with

$$p_0^2(x) = Q_0(x), \quad p_1(x) = -\frac{p'_0(x)}{2p_0(x)}, \quad p_2(x) = -\frac{1}{2p_0(x)} (p_1^2(x) + p'_1(x) - Q_2(x)).$$

The odd and even power of $P(x, \hbar)$

$$P_{\text{even}}(x, \hbar) = \sum_0^{\infty} p_{2n}(x)\hbar^{2n}, \quad P_{\text{odd}}(x, \hbar) = \sum_0^{\infty} p_{2n+1}(x)\hbar^{2n+1}, \quad (2.7)$$

was proven splitting by

$$P_{\text{odd}}(x, \hbar) = -\frac{\hbar}{2} \frac{d}{dx} \log P_{\text{even}}(x, \hbar). \quad (2.8)$$

Hereafter we omit \hbar dependent in function $P(x, \hbar)$ for short. Then the WKB solution (2.3) can be expressed in terms of $P_{\text{even}}(x)$ as

$$\psi_a^{\pm}(x) = \frac{1}{\sqrt{P_{\text{even}}(x)}} \exp\left(\pm \frac{1}{\hbar} \int_a^x P_{\text{even}}(x) dx\right), \quad (2.9)$$

where a is a reference point for the integral, and is often exclusively chosen to be a turning point, that satisfies $Q_0(a) = 0$. The prescription \pm in the exponential signifies the properties of the solutions, exponentially suppressed, exponentially growing, or oscillatory in the given region of x . The generic solution normalized at a consists of the linear combination of two independent components $\psi_a^{\pm}(x)$

$$\psi_a(x) = \frac{C_+}{\sqrt{P_{\text{even}}(x)}} \exp\left(\frac{1}{\hbar} \int_a^x P_{\text{even}}(x) dx\right) + \frac{C_-}{\sqrt{P_{\text{even}}(x)}} \exp\left(-\frac{1}{\hbar} \int_a^x P_{\text{even}}(x) dx\right). \quad (2.10)$$

One can formally include the all-order quantum corrections into the wave function by expanding (2.9) to orders of \hbar

$$\psi_a^{\pm}(x) = \exp\left(\pm \frac{1}{\hbar} \int_a^x p_0(x) dx\right) \sum_{n=0}^{\infty} \psi_{a,n}^{\pm}(x) \hbar^n. \quad (2.11)$$

Hereafter, we specify $p_0(x) = \sqrt{Q_0(x)}$. This formal series includes an exponential prefactor and formal power series with its coefficients x -dependent. It is of course divergent in general. The Borel resummation provides a procedure to deal with this sort of divergent series, next we will consider its utilization into formal series (2.11).

2.2 Stokes graphs and connection formulas

2.2.1 Borel resummation and Stokes graphs

We consider a generic form of formal series with exponential prefactor, which appears at the formal expansion of the WKB solution for wave function (2.11)

$$f(\hbar) = e^{-\frac{A}{\hbar}} \sum_{n=0}^{\infty} a_n \hbar^{n+\alpha}, \quad \alpha \notin \{-1, -2, -3, \dots\}, \quad (2.12)$$

where A is a constant independent of \hbar and a_n diverges factorially $a_n \sim n!$. Its Borel transform is

$$\mathcal{B}[f](z) = \sum_{n=0}^{\infty} \frac{a_n}{\Gamma(n+\alpha)} (z-A)^{n+\alpha-1}, \quad (2.13)$$

which transforms the divergent formal series (2.12) into a well-defined function in the new variable z . This function has a finite convergent radius and can be analytically continued to a domain including the real z -axis, with possible singularities, such as poles. We often call this complex z -plane the Borel plane. If there is no singularity along the positive real line, one can define the Laplace transform of Borel-transformed function $\mathcal{B}[f](z)$ as

$$\mathcal{S}[f](\hbar) = \mathcal{L}[\mathcal{B}[f](z)] = \int_A^{\infty} dz e^{-\frac{z}{\hbar}} \mathcal{B}[f](z), \quad (2.14)$$

it is the Borel resummation or simply Borel resum of the original formal series (2.12), and we say the formal series (2.12) is Borel summable in this case. The directional Borel resum can be defined similarly if there is no singularity in angle θ

$$\mathcal{S}_{\theta}[f](\hbar) = \mathcal{L}_{\theta}[\mathcal{B}[f](z)] = \int_A^{e^{i\theta}\infty} dz e^{-\frac{z}{\hbar}} \mathcal{B}[f](z). \quad (2.15)$$

One may note this sort of directional summation is equivalent to writing as

$$\mathcal{S}_\theta[f](\hbar) = \mathcal{S}_0[f](e^{i\theta}\hbar), \quad (2.16)$$

which indicates the Borel resum for formal series at the angle θ is equivalent to the resum at angle 0 by rotating \hbar to $e^{i\theta}\hbar$. We will omit the subscript 0 in \mathcal{S}_θ when $\theta = 0$. It is much more fruitful to look at the singularities in the Borel plane, let us simply consider there is a single pole along θ ray, then the integral defined in (2.15) makes no sense. But we can bypass the pole by small derivation from above and below, this suggests defining the lateral Borel resum for (2.12) as

$$\mathcal{S}_{\theta\pm}[f](\hbar) = \lim_{\delta \rightarrow 0} \mathcal{L}_{\theta\pm\delta}[\mathcal{B}[f](z)]. \quad (2.17)$$

Let us now consider the formal series expansion for wave function (2.11), we will study its Borel singularities and Borel summability. The general Borel resum procedure is applicable, but the expansion coefficients $\psi_{a,n}^\pm$ are parameter-dependent on x . This parameter-dependence promotes the singularities in the Borel plane to be x dependent and then defines curves in coordinate x plane, that is Stokes lines introduced later. At first, We do Borel transform of (2.11) to suppress the divergence

$$\mathcal{B}[\psi_a^\pm(x)](z) = \sum_{n=0}^{\infty} \frac{\psi_{a,n}^\pm(x)}{\Gamma(n)} (z \pm z_0)^{n-1}, \quad z_0 = \frac{1}{\hbar} \int_a^x p_0(x) dx. \quad (2.18)$$

Now we obtain a convergent function defined in some domain in the z -plane, it is generally meromorphic with possible singularities and one can further continue the function into the whole z -plane. Its Laplace transform can be defined accordingly unless the integral contour encounters Borel poles.

$$\mathcal{S}_\theta[\psi_a^\pm](\hbar) = \int_{\mp z_0}^{e^{i\theta}\infty} e^{-\frac{z}{\hbar}} \mathcal{B}[\psi_a^\pm(x)](z) dz, \quad \theta = \arg(\hbar). \quad (2.19)$$

Figure 2.1 shows the definition of $\mathcal{S}_\theta[\psi_a^+](\hbar)$ for $\theta = 0$. Hereafter we will use $\psi_a^\pm(x)$ to represent Borel-resummed wave functions for simplicity without confusion. It is proved that $\pm z_0(x)$ are singular points of the Borel transform (2.18) [18]. The location of $\pm z_0(x)$

depends on the coordinate x , so the integral contour is able to touch the Borel pole $z_0(x)$ in figure 2.1 by moving in the complex x plane. This condition can be expressed as

$$\text{Im} \frac{1}{\hbar} \int_a^x p_0(x) dx = 0, \quad (2.20)$$

which defines Stokes lines eliminating from a turning point a . Moreover, the real part tells us which one in $\psi_a^\pm(x)$ is growing or decreasing, so we attach each line $+$ or $-$ to specify the behavior of solutions. It's determined by the sign of the following quantity

$$\text{Re} \frac{1}{\hbar} \int_a^x p_0(x) dx. \quad (2.21)$$

The positive value indicates $\psi^+(x)$ increases exponentially, while $\psi^-(x)$ decreases exponentially. If it's negative, $\psi^-(x)$ increases while $\psi^+(x)$ decreases.

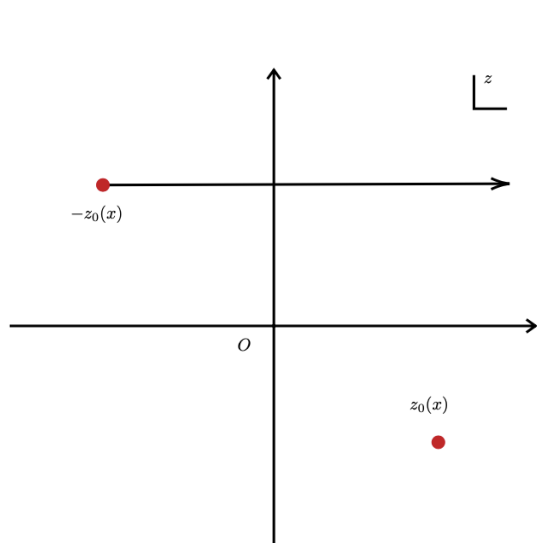


Figure 2.1: This is the Borel plane for Borel transform of $\psi_a^+(x)$. The arrow represents the integral contour for $\theta = 0$. The right red point denotes the corresponding Borel pole.

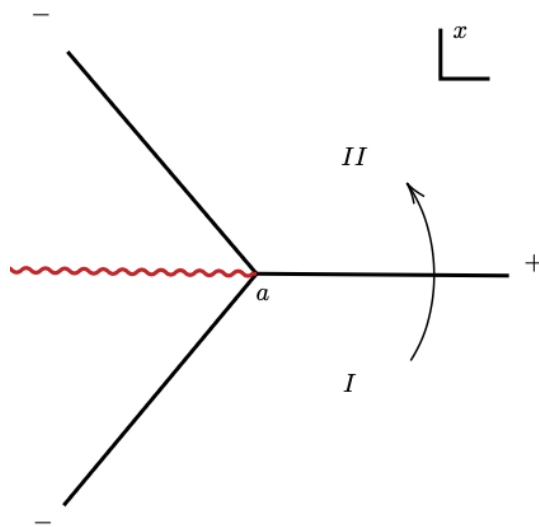


Figure 2.2: This figure shows the Stokes lines eliminating from a simple turning point a . \pm labels the orientations of Stokes lines. The arrow states the continuation path from Stokes region I to II and the red wavy line is branch cut.

For each turning point, one can define the corresponding Stokes lines, and there are three Stokes lines for a simple turning point, i.e. the simple zero of $Q_0(x)$. Figure 2.2 shows the Stokes lines eliminating from simple turning point a to complex infinity. One Stokes line might start from one turning point, the origin, or infinity and end at another turning point, the origin or infinity. The Stokes line connecting two turning points is a degenerate line and can be resolved by saddle reduction via introducing a small derivation for integral contour $\theta \rightarrow \theta \pm \delta$.

The Stokes lines divide the coordinate plane into several adjacent regions, usually called Stokes regions. The collection of all the Stokes lines composes Stokes graphs. Within each Stokes region, the formal series for wave functions is Borel summable to obtain the analytic solution for each region. However, if one continues the solution in one region to another adjacent region by crossing a Stokes line, one of the components in ψ^\pm gets a discontinuity while the other one remains depending on the orientation of the Stokes line. This is quantitatively described by the connection formula in the subsequent section.

2.2.2 Connection formulas and quantum periods

We know Borel singularities for wave functions, which are captured by Stokes curves qualitatively, now we want to know the quantitative discontinuities when the wave functions in one Stokes region cross the Stokes line to an adjacent region. In general, this property is concluded by the following connection formula [20, 23].

- If crossing a Stokes line anticlockwise at which the ψ^+ is dominant, ψ^+ gains a discontinuity controlled by ψ^- , while ψ^- doesn't change,

$$\psi^+ \rightarrow \psi^+ + i\psi^-, \quad \psi^- \rightarrow \psi^-, \quad (2.22)$$

As aforementioned, the symbol for the Borel resum is omitted.

- If crossing the Stokes line anticlockwise at which the ψ^- is dominant, ψ^- gains a

discontinuity controlled by ψ^+ , while ψ^+ remains unchanged,

$$\psi^- \rightarrow \psi^- + i\psi^+, \quad \psi^+ \rightarrow \psi^+, \quad (2.23)$$

- If crossing a Stokes line clockwise, the formulas differ by flipping the $+$ to $-$ in front of the i ,
- If crossing a branch cut emerging from a turning point anti-clockwise (clockwise), the dominant and subdominant component exchange (with a minus sign),

$$\psi^+ \rightarrow \pm\psi^-, \quad \psi^- \rightarrow \pm\psi^+, \quad + \text{ for anticlockwise, } - \text{ for clockwise.} \quad (2.24)$$

One usually signs the corresponding matrix to represent this formulation

$$M_+ = \begin{pmatrix} 1 & i \\ 0 & 1 \end{pmatrix}, \quad M_- = \begin{pmatrix} 1 & 0 \\ i & 1 \end{pmatrix}, \quad (2.25)$$

which is often called the monodromy matrix. Then the connection formulas can be stated that the WKB solutions in one Stokes region can be obtained via multiplication of the monodromy matrix by the solutions in the adjacent region, specifically

$$\begin{pmatrix} \psi_{a,I}^+ \\ \psi_{a,I}^- \end{pmatrix} = M \begin{pmatrix} \psi_{a,II}^+ \\ \psi_{a,II}^- \end{pmatrix}, \quad (2.26)$$

which is represented in figure 2.2 where $M = M_+$.

Furthermore, the two independent wave functions normalized in a turning point a_1 denoted as $\psi_{a_1}^\pm$, and $\psi_{a_2}^\pm$ normalized in another turning point a_2 are related by normalization coefficients $N_{a_1 a_2}^\pm$ defined as

$$N_{a_1 a_2}^\pm = \exp\left(\pm \frac{1}{\hbar} \int_{a_1}^{a_2} P_{\text{even}}(x) dx\right), \quad (2.27)$$

which induces the following connection formula to relate wave functions normalized in a_2 to a_1

$$\psi_{a_1}^\pm(x) = N_{a_1 a_2}^\pm \psi_{a_2}^\pm(x). \quad (2.28)$$

In the latter context, we will intensively use the following notation

$$\mathcal{V}_\gamma \equiv \exp \left(\frac{1}{\hbar} \oint_\gamma P_{\text{even}}(x) dx \right), \quad (2.29)$$

where γ is the cycle encircling two turning points a_1 and a_2 . It is usually called Voros multipliers or Voros symbols in the literature. As the same as the monodromy matrix, we can express the above connection formula in a matrix form, which transforms the wave function basis at turning point a_2 to a_1

$$\begin{pmatrix} \psi_{a_1}^+(x) \\ \psi_{a_1}^-(x) \end{pmatrix} = N_{a_1 a_2} \begin{pmatrix} \psi_{a_2}^+(x) \\ \psi_{a_2}^-(x) \end{pmatrix}, \quad N_{a_1 a_2} = \begin{pmatrix} \mathcal{V}_\gamma^{\frac{1}{2}} & 0 \\ 0 & \mathcal{V}_\gamma^{-\frac{1}{2}} \end{pmatrix}. \quad (2.30)$$

At the equal significance, we rename the quantity $\oint_\gamma P_{\text{even}}(x) dx$ the quantum period or quantum WKB period corresponding to the cycle γ

$$\Pi_\gamma(\hbar) = \oint_\gamma P_{\text{even}}(x) dx. \quad (2.31)$$

It's now necessary to re-explain notations. Corresponding to (2.1), there exists a classical curve

$$y^2 = Q_0(x), \quad (2.32)$$

it is called the WKB curve. Geometrically it defines a Riemann surface Σ_{WKB} , and the quantum period is the integral of meromorphic differential $P_{\text{even}}(x) dx$ along the one-cycle $\gamma \in H_1(\Sigma_{\text{WKB}})$. The leading order of the quantum period is often called the classical WKB period or classical period

$$\Pi_\gamma^{(0)} \equiv \oint_\gamma p_0(x) dx, \quad (2.33)$$

which plays an important role in the history of quantum mechanics. The well-known Bohr-Sommerfeld (BS) quantization condition can be written in terms of the classical period as

$$\Pi_\gamma^{(0)} = 2\pi i \hbar \left(n + \frac{1}{2} \right), \quad n = 0, 1, 2, \dots, \quad (2.34)$$

where γ is specified to be one cycle around the classically allowed region. It is widely used for two-turning-point problems by accounting for the classical period integral encircling turning points a_1 and a_2 in the classically allowed region. Here i appears since

our notation for $p_0(x) = \sqrt{V(x) - E}$, which is different from the conventional choice $p_0(x) = \sqrt{E - V(x)}$.

We should carefully note $P_{\text{even}}(x)$ is defined asymptotically by recursive relation, so Voros symbols and also quantum periods are divergent formal series of \hbar , for instance

$$\Pi_\gamma(\hbar) = \oint_\gamma \left(\sum_{n \in \mathbb{N}} p_{2n}(x, \hbar) \hbar^{2n} \right) dx \sim \sum_{n \in \mathbb{N}} \Pi_\gamma^{(n)} \hbar^{2n}, \quad (2.35)$$

with its coefficient diverging double-factorially

$$\Pi_\gamma^{(n)} \sim (2n)!. \quad (2.36)$$

Since the WKB solutions in (2.28) are resummed well-defined functions. One should regard the Voros symbols and quantum periods as Borel-resummed quantities, but we will omit the notation of Borel resummation \mathcal{S} for short.

Until now, we have introduced Stokes graphs which are fully determined by the classical potential $Q_0(x)$, and connection formulas based on the all-orders wave function and its Borel summability. With these ingredients, we are able to analytically continue the WKB solution defined in one Stokes region to another region and rewrite the solutions in one Stokes region as the linear combination of the wave basis for another region. In the content of WKB analysis, these combination coefficients rely on Voros symbols. In practice, proper boundary conditions are imposed for interested problems, which give an additional condition for these coefficients. The equality that fulfills boundary conditions is called the exact quantization condition, which is a functional relation in terms of Voros symbols as follows

$$\mathcal{Q}(\mathcal{V}_{\gamma_1}, \dots, \mathcal{V}_{\gamma_r}) = 0, \quad (2.37)$$

where \mathcal{V}_{γ_i} with $i = 1, 2, \dots, r$ are Voros symbols on the relevant one-cycle γ_i . For example, the EQC for harmonic oscillator can be written as

$$1 + \mathcal{V}_\gamma = 0, \quad (2.38)$$

which is the BS quantization condition (2.34). We intend to drive the EQCs for the Stark problem in the next section by following the above strategy.

3 Stark Effect and its quantization conditions

Let us first write down the Schrödinger equation for the stark effect of hydrogen in a uniform electric field F oriented in the z -axis:

$$\left(-\frac{\hbar^2}{2}\nabla^2 - \frac{1}{r} + Fz\right)\Psi = E\Psi, \quad (3.1)$$

where atomic units are adopted, and E represents the energy. r denotes the radial coordinate. We remain reduced Planck constant \hbar , which is set to 1 in the end.

3.1 Langer's modification and boundary conditions

We introduce the parabolic coordinates (ξ, η, φ) which are defined by

$$\begin{aligned} x + iy &= \sqrt{\xi\eta}e^{i\varphi}, & \xi &= r + z, \\ z &= \frac{1}{2}(\xi - \eta), & \eta &= r - z, \\ r &= \frac{1}{2}(\xi + \eta), & \tan\varphi &= \frac{y}{x}, \end{aligned} \quad (3.2)$$

where $r = \sqrt{x^2 + y^2 + z^2}$, $0 \leq \xi, \eta \leq +\infty$ and $0 \leq \varphi \leq 2\pi$. If we consider an ansatz for wave function Ψ as

$$\Psi = \frac{1}{\sqrt{\xi\eta}}\psi_1(\xi)\psi_2(\eta)e^{im\varphi}, \quad (3.3)$$

the three-dimensional Schrödinger equation (3.1) reduces to a couple of Schrödinger-like equations with centrifugal term

$$\begin{aligned} \left(-\hbar^2\frac{d^2}{d\xi^2} + \frac{F}{4}\xi - \frac{E}{2} - \frac{A_1}{\xi} + \frac{\hbar^2(m^2 - 1)}{4\xi^2}\right)\psi_1(\xi) &= 0, \\ \left(-\hbar^2\frac{d^2}{d\eta^2} - \frac{F}{4}\eta - \frac{E}{2} - \frac{A_2}{\eta} + \frac{\hbar^2(m^2 - 1)}{4\eta^2}\right)\psi_2(\eta) &= 0, \end{aligned} \quad (3.4)$$

where A_1 and A_2 are separation constants satisfying $A_1 + A_2 = 1$. One can identify the parameters above with that of potential in the standard form (2.1) with

$$Q_0(x) = u_0x + u_1 + \frac{u_2}{x}, \quad Q_2(x) = \frac{\ell(\ell + 1)}{x^2}, \quad (3.5)$$

to find

$$Q_0(x) = \frac{F}{4}x - \frac{E}{2} - \frac{A_1}{x}, \quad \text{or} \quad Q_0(x) = -\frac{F}{4}x - \frac{E}{2} - \frac{A_2}{x}, \quad (3.6)$$

for the equation corresponding to ξ and η coordinates respectively. In both cases, orbital quantum number ℓ and azimuthal quantum number m are related by

$$\left| \ell + \frac{1}{2} \right| = \left| \frac{m}{2} \right|. \quad (3.7)$$

It is proven that the above equations are appropriate to the WKB analysis including all-order expansions, however, they are not capable to grasp the leading order contribution to the wave function properly. We use the generalization of the Kramers-Langer substitution [8, 9] by

$$\hbar^2 \ell(\ell + 1) \rightarrow \hbar_i^2 \left(\ell + \frac{1}{2} \right)^2 - \frac{\hbar^2}{4}, \quad (3.8)$$

or in terms of m as

$$\frac{\hbar^2(m^2 - 1)}{4} \rightarrow \frac{\hbar_i^2 m^2}{4} - \frac{\hbar^2}{4}. \quad (3.9)$$

Here another parameter \hbar_i is introduced as an implicit factor, while \hbar is an explicit expansion parameter. The different partitions of the centrifugal term as above represent different expansion schemes but give the same physical solution when $\hbar_i = \hbar$. The WKB expansions for (3.9) do not match term by term except for the first order and infinite order, see [9] for detailed discussion. Since \hbar_i is not involved in power expansions, we can directly set it to 1 at the beginning. This generalized Langer's modification suggests splitting the centrifugal term into two parts as

$$\begin{aligned} \left(-\hbar^2 \frac{d^2}{d\xi^2} + \frac{F}{4}\xi - \frac{E}{2} - \frac{A_1}{\xi} + \frac{m^2}{4\xi^2} - \frac{\hbar^2}{4\xi^2} \right) \psi_1(\xi) &= 0, \\ \left(-\hbar^2 \frac{d^2}{d\eta^2} - \frac{F}{4}\eta - \frac{E}{2} - \frac{A_2}{\eta} + \frac{m^2}{4\eta^2} - \frac{\hbar^2}{4\eta^2} \right) \psi_2(\eta) &= 0. \end{aligned} \quad (3.10)$$

Now we can set

$$Q_0(\xi) = \frac{F}{4}\xi - \frac{E}{2} - \frac{A_1}{\xi} + \frac{m^2}{4\xi^2}, \quad Q_2(\xi) = -\frac{1}{4\xi^2}, \quad (3.11)$$

for ξ coordinate and

$$Q_0(\eta) = -\frac{F}{4}\eta - \frac{E}{2} - \frac{A_2}{\eta} + \frac{m^2}{4\eta^2}, \quad Q_2(\eta) = -\frac{1}{4\eta^2}, \quad (3.12)$$

for η coordinate. Let us then check the behaviors of the wave functions at the boundaries. It is enough to take account of the leading order WKB solution of (2.9) at this stage

$$\psi(x) \sim \frac{1}{\sqrt{p_0(x)}} \exp\left(\pm \frac{1}{\hbar} \int_a^x p_0(x) dx\right). \quad (3.13)$$

We temporarily set $\hbar = 1$ for clarity, and consider the ξ -equation at first. Near the origin, the inverse square term dominates the wave function

$$Q_0(\xi) \sim \frac{m^2}{4\xi^2}, \quad p_0(\xi) \sim \frac{|m|}{2} \frac{1}{\xi}. \quad (3.14)$$

Then the wave function near the origin behaves like

$$\psi_1^\pm(\xi) \sim \frac{1}{\sqrt{p_0(\xi)}} \exp\left(\pm \int^\xi p_0(\xi) d\xi\right) \sim \xi^{\frac{1}{2} \pm \frac{|m|}{2}} \sim \begin{cases} \xi^{\ell+1}, & \text{for } +, \\ \xi^{-\ell}, & \text{for } -, \end{cases} \quad (3.15)$$

where (3.7) is used at the last step. We then obtain one normalizable solution $\psi_1^+(\xi)$, that is proper for the Stark problem, and one divergent solution $\psi_1^-(\xi)$. Now let us turn to consider the behavior of the solution at infinity, the dominant contribution to $p_0(\xi)$ is

$$Q_0(\xi) \sim \frac{F}{4}\xi, \quad p_0(\xi) \sim \frac{F}{2}\xi^{\frac{1}{2}}. \quad (3.16)$$

It is obvious to find the following asymptotic approximation

$$\psi_1^\pm(\xi) \sim \xi^{-\frac{1}{4}} e^{\pm \frac{F}{3}\xi^{\frac{3}{2}}}. \quad (3.17)$$

We get one increasing solution and one exponentially suppressed solution, the latter is what we expect, namely $\psi_1^-(\xi)$ at the asymptotic infinite region. The wave function for the η -equation can be analyzed in the same way. Near the origin, it is entirely the same as that for the ξ -equation.

$$\psi_2^\pm(\eta) \sim \frac{1}{\sqrt{p_0(\eta)}} \exp\left(\pm \int^\eta p_0(\eta) d\eta\right) \sim \eta^{\frac{1}{2} \pm \frac{|m|}{2}} \sim \begin{cases} \eta^{\ell+1}, & \text{for } +, \\ \eta^{-\ell}, & \text{for } -. \end{cases} \quad (3.18)$$

The boundary condition requires the ψ_2^+ component to survive. At large η region, the dominant part for $p_0(\eta)$ changes to

$$Q_0(\eta) \sim -\frac{F}{4}\eta, \quad p_0(\eta) \sim i\frac{F}{2}\eta^{\frac{1}{2}}, \quad (3.19)$$

then the wave function asymptotically behaves like

$$\psi_2^\pm(\eta) \sim \eta^{-\frac{1}{4}} e^{\pm i\frac{F}{3}\eta^{\frac{3}{2}}}. \quad (3.20)$$

This time we obtain one outgoing wave $\psi_2^+(\eta)$ and one ingoing wave $\psi_2^-(\eta)$, the former satisfies the required boundary condition.

Then we are going to apply connection formulas in section 2 to relate the wave functions from one Stokes region to another region and impose the above boundary conditions, which generates a functional relation for the quantum periods and gives us exact quantization conditions for the Stark problem.

3.2 Quantization conditions

The quantization conditions can be derived from the Stokes graphs incorporating boundary conditions discussed in the last section. For equations (3.10), there are three turning points a , b , and c when $m \neq 0$. $m = 0$ is a special case, we deal with it by taking a limit as explained in the later calculation. One can plot the Stokes lines starting from each turning point by solving condition (2.20). The Stokes graph can be established by combining all the Stokes lines in the complex ξ or η coordinate plane. Typical graphs are shown in figure 3.1.

Let us first consider the ξ -equation, we find the interesting phenomenon that the Stokes graph changes its topology when field strength F increases for fixed m . The critical condition for this transition is characterized by

$$\text{Im} \frac{1}{\hbar} \int_b^c \sqrt{Q_0(\xi)} d\xi = 0, \quad (3.21)$$

where one Stokes line connects two turning points b and c , and it becomes degenerate. This condition is actually really involved, since $E, A_{1,2}$ do depend on F and m in the potential

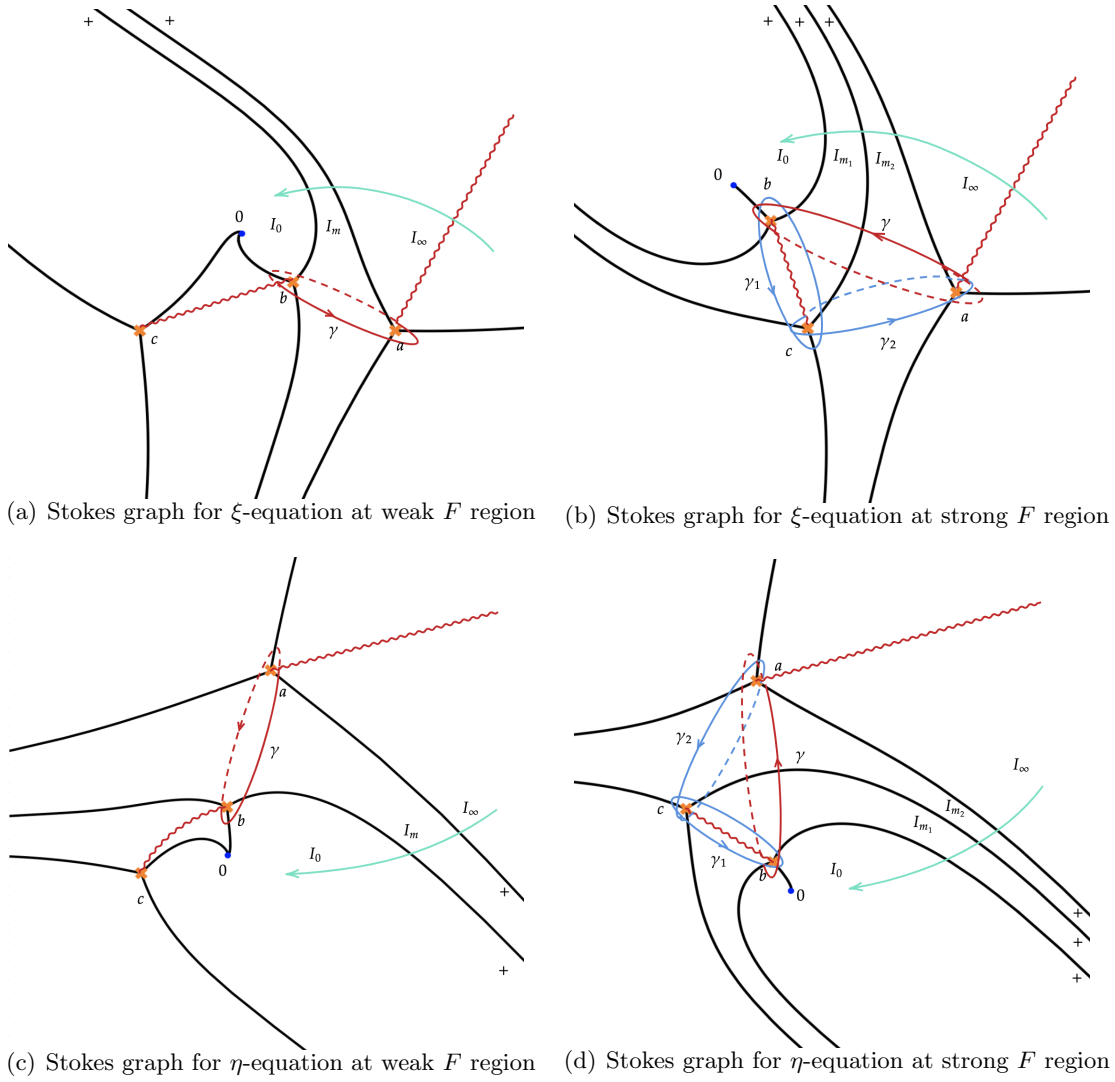


Figure 3.1: Stokes graphs and its transition. The orange cross denotes three turning points a , b , and c respectively. The blue point is the origin. The red wavy lines are branch cuts and the green arrow represents the continuation path. γ , γ_1 , and γ_2 are one-cycle encircling turning points, dashed lines indicate the contour enters the second sheet after crossing a branch cut. The Stokes lines are represented by black lines with $+$ and $-$ indicating the orientation. I_0 , I_m , and I_∞ are adjacent Stokes regions.

(3.11). These four parameters are not independent. E and $A_{1,2}$ are determined when specifying F and m . We regard F and m as free parameters in the potential, and then the transition condition (3.21) divides the space of parameter (F, m) into two distinct regions. We name these two regions weak F region with smaller F and strong F region with larger F . We use $F_{\xi,c}(m)$ to denote this critical value for a given m . There is no simple way to determine this value explicitly to our best knowledge. In principle, one can figure out the corresponding Stokes graph for specified F and m with E and $A_{1,2}$ determined by other methods to confirm which region it belongs to. For instance, $F_{\xi,c}(1) \in (0.3, 0.4)$.

Let us now focus on the Stokes graph for the ξ -equation in the weak F region, its Stokes graph is shown in figure 1(a). To derive the quantization condition, we have to know the relation of wave functions between origin and infinity, which can be accomplished by using connection formulas in section 2. One can continue the solutions at infinity to the origin along the green arrow depicted in figure 1(a), this procedure can be written as follows.

1. We start from the wave function basis in Stokes region I_∞ normalized at a , it is necessary at first to cross the branch cut which exchanges the exponentially suppressed and growing solutions, this progress can be written as

$$\begin{pmatrix} \iota\psi_{a,I_\infty}^-(\xi) \\ \iota\psi_{a,I_\infty}^+(\xi) \end{pmatrix} = \begin{pmatrix} \psi_{a,I_\infty}^+(\xi) \\ \psi_{a,I_\infty}^-(\xi) \end{pmatrix}, \quad (3.22)$$

where the operator ι maps the function in one square sheet to one in another sheet.

2. Now we are working in the same sheet, we continue the wave functions $\psi_{a,I_\infty}^\pm(\xi)$ to cross the Stokes line labeled by $+$ anticlockwise to get basis in the intermediate region I_m normalized at the same turning point a by the multiplication of the monodromy matrix M_+

$$\begin{pmatrix} \psi_{a,I_\infty}^+(\xi) \\ \psi_{a,I_\infty}^-(\xi) \end{pmatrix} = M_+ \begin{pmatrix} \psi_{a,I_m}^+(\xi) \\ \psi_{a,I_m}^-(\xi) \end{pmatrix}. \quad (3.23)$$

3. We obtain the basis in the region I_m normalized at a , to continue the procedure along the green line, it's necessary to arrive at the basis normalized at b for the same Stokes

region I_m . It is accomplished by the normalization matrix

$$\begin{pmatrix} \psi_{a,I_m}^+(\xi) \\ \psi_{a,I_m}^-(\xi) \end{pmatrix} = N_{ab} \begin{pmatrix} \psi_{b,I_m}^+(\xi) \\ \psi_{b,I_m}^-(\xi) \end{pmatrix}. \quad (3.24)$$

4. As the same as the second step, by crossing a Stokes line labeled by $+$ anticlockwise, one gets the basis in the region I_0 normalized at b

$$\begin{pmatrix} \psi_{b,I_m}^+(\xi) \\ \psi_{b,I_m}^-(\xi) \end{pmatrix} = M_+ \begin{pmatrix} \psi_{b,I_0}^+(\xi) \\ \psi_{b,I_0}^-(\xi) \end{pmatrix}. \quad (3.25)$$

5. We finally pull back the normalization from b to a for comparison.

$$\begin{pmatrix} \psi_{b,I_0}^+(\xi) \\ \psi_{b,I_0}^-(\xi) \end{pmatrix} = N_{ba} \begin{pmatrix} \psi_{a,I_0}^+(\xi) \\ \psi_{a,I_0}^-(\xi) \end{pmatrix}. \quad (3.26)$$

Accounting for all these transformations, it's apparent the two bases are related by the matrix multiplication as

$$\begin{pmatrix} \nu\psi_{a,I_\infty}^-(\xi) \\ \nu\psi_{a,I_\infty}^+(\xi) \end{pmatrix} = M_+ N_{ab} M_+ N_{ba} \begin{pmatrix} \psi_{a,I_0}^+(\xi) \\ \psi_{a,I_0}^-(\xi) \end{pmatrix} = \begin{pmatrix} \psi_{a,I_0}^+(\xi) + i(1 + \mathcal{V}_\gamma)\psi_{a,I_0}^-(\xi) \\ \psi_{a,I_0}^-(\xi) \end{pmatrix}, \quad (3.27)$$

here \mathcal{V}_γ is the Voros symbol, and γ is the trajectory enclosing turning points b and a . This expression relates the wave function basis at positive infinity to that around the origin. We note that this formula is very similar to the Q-function in the ODE/IM correspondence [27] and also the numerical method used in [5, 6]. The boundary conditions for (3.15) and (3.17) require ψ_{a,I_0}^- and $\nu\psi_{a,I_\infty}^+$ to vanish, which deduce the following quantization condition

$$\mathcal{Q}(\mathcal{V}_\gamma) := 1 + \mathcal{V}_\gamma = 1 + \exp\left(\frac{1}{\hbar} \oint_\gamma P_{\text{even}}(\xi) d\xi\right) = 0. \quad (3.28)$$

We can then write down the Bohr-Sommerfeld-type quantization condition

$$\Pi_\gamma(\hbar) = \oint_\gamma P_{\text{even}}(\xi) d\xi = 2\pi i \hbar \left(n_\xi + \frac{1}{2}\right), \quad n_\xi = 0, 1, 2, \dots, \text{ for small } F \text{ region}, \quad (3.29)$$

where n_ξ denotes the quantum number corresponding to ξ coordinate. Let us emphasize that the left side quantum periods should be understood as its Borel resum. This quantization condition was presented for the Stark problem a long time ago such as [12], where the leading order contribution is considered. Here we derive it rigorously and show it is exactly satisfied when taking quantum correction into consideration. Then this Bohr-Sommerfeld quantization condition for the Borel-resummed quantum periods provides the exact condition.

Next, we turn our attention to the Stokes graph for ξ -equation with a strong F . The Stokes graph changes its topology when F is enlarged, as described in figure 1(a) and 1(b). We follow a similar process as discussed before. the connection of the solutions from infinity to the origin for 1(b) is given by the matrix multiplication

$$\begin{pmatrix} \iota\psi_{a,I_\infty}^-(\xi) \\ \iota\psi_{a,I_\infty}^+(\xi) \end{pmatrix} = M_+ N_{ac} M_+ N_{cb} M_+ N_{bc} N_{ca} \begin{pmatrix} \psi_{a,I_0}^+(\xi) \\ \psi_{a,I_0}^-(\xi) \end{pmatrix} = \begin{pmatrix} \psi_{a,I_0}^+(\xi) + i(1 + \mathcal{V}_{\gamma_2} + \mathcal{V}_{\gamma_1} \mathcal{V}_{\gamma_2})\psi_{a,I_0}^-(\xi) \\ \psi_{a,I_0}^-(\xi) \end{pmatrix}, \quad (3.30)$$

Then the boundary condition requires

$$\mathcal{Q}(\mathcal{V}_\gamma, \mathcal{V}_{\gamma_1}) := 1 + \mathcal{V}_\gamma + \mathcal{V}_{\gamma_2} = 1 + \mathcal{V}_\gamma (1 + \mathcal{V}_{\gamma_1}^{-1}) = 0, \quad (3.31)$$

which is the exact quantization condition for the large F region. where we use the fact

$$\Pi_{\gamma_1} + \Pi_{\gamma_2} = \Pi_\gamma \quad \text{or} \quad \mathcal{V}_{\gamma_1} \mathcal{V}_{\gamma_2} = \mathcal{V}_\gamma. \quad (3.32)$$

We can write the quantization condition of the modified Bohr-Sommerfeld type from (3.31) as

$$\Pi_\gamma(\hbar) + \log \left(1 + e^{-\frac{1}{\hbar} \Pi_{\gamma_1}(\hbar)} \right) = 2\pi i \hbar \left(n_\xi + \frac{1}{2} \right), \quad n_\xi = 0, 1, 2, \dots, \quad \text{for large } F \text{ region.} \quad (3.33)$$

Here $\Pi_\gamma(\hbar)$ and $\Pi_{\gamma_1}(\hbar)$ are also Borel-resummed quantities. It was found that \mathcal{V}_{γ_1} gives an exponentially suppressed contribution, so the BS quantization condition still gives an approximation in the small \hbar limit. The additional logarithmic term plays a role of non-perturbative correction, which becomes significant when F is large.

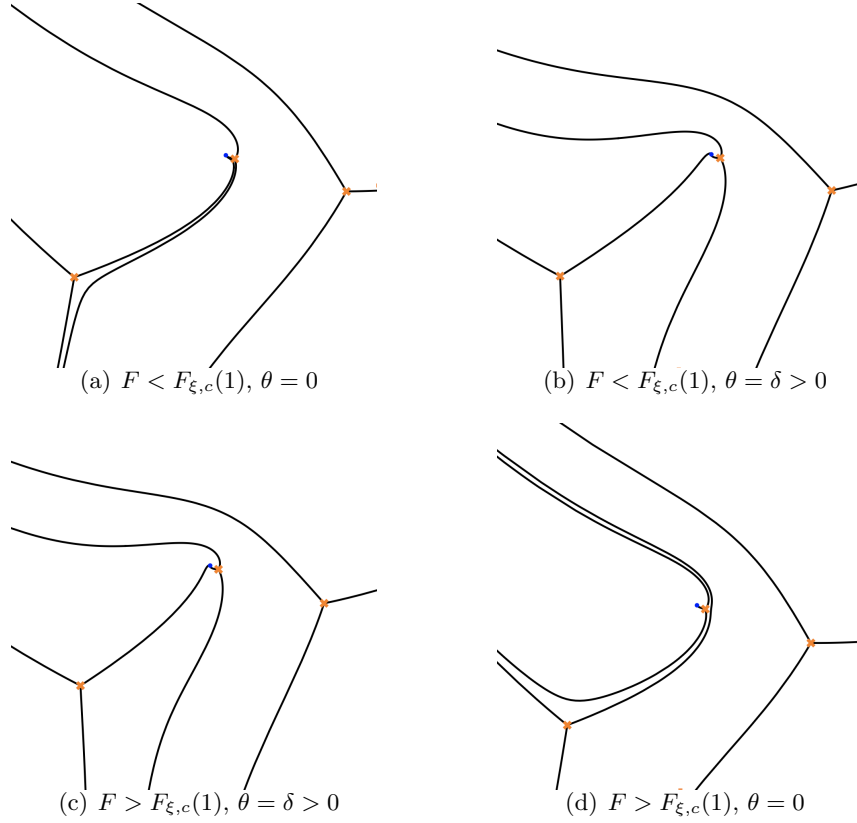


Figure 3.2: The transition of Stokes graphs for ξ -equation with rotating $\theta = \arg(\hbar)$.

One may wonder about the continuity of the EQCs (3.29) and (3.33), which is clarified by the saddle reduction of Stokes graphs. It is proven the saddle reduction induced by (3.21) is equivalent to the rotation of \hbar . Figure 3.2 shows the transition of Stokes graphs for ξ equation by tuning F and rotating $\theta = \arg(\hbar)$. One starts from a Stokes graph for $F < F_{\xi,c}(1)$ with $\arg(\hbar) = 0$ and $m = 1$ fixed, its mutation by rotating \hbar with a small δ does not change the configuration of the Stokes graph as indicated in figure 2(a) and 2(b). The Stokes graph moves to figure 2(c) continuously by increasing F with $\arg(\hbar)$ fixed. Then as we continuously change $\arg(\hbar)$ to 0 with F fixed, the Stokes graph becomes figure 2(d). During this process, turning points b and c are connected by one Stokes line at an angle φ with $0 < \varphi < \delta$. And quantum period $\Pi_\gamma(\hbar)$ exhibits singularities in its Borel plane at

direction φ , the discontinuity of the quantum period is given by the Delabaere-Pham (DP) formula [25]

$$\exp\left(\frac{1}{\hbar}\mathcal{S}_+[\Pi_\gamma]\right) = \exp\left(\frac{1}{\hbar}\mathcal{S}_-[\Pi_\gamma]\right) \left(1 + \exp\left(-\frac{1}{\hbar}\mathcal{S}[\Pi_{\gamma_1}]\right)\right), \quad (3.34)$$

here \mathcal{S}_\pm are two lateral Borel summations for $\theta = 0$ defined in section 2. The DP formula shows the EQC or complex resonant frequency is continuous during the transition of the Stokes graphs. Furthermore, it gives the resurgent structure of the quantum periods which indicates the discontinuity of the perturbative contribution is governed by the non-perturbative term. See [36, 37] for a similar discussion.

The derivation of quantization conditions for η -equation is parallel to the above analysis, the critical condition for the mutation of the Stokes graph is given by

$$\text{Im} \frac{1}{\hbar} \int_b^c \sqrt{Q_0(\eta)} d\eta = 0, \quad (3.35)$$

which divides parameters in the potential into the weak F region and the strong F region accordingly. We can similarly denote $F_{\eta,c}(m)$ as the critical value of the transition for fixed m , an estimation for $m = 1$ implies $F_{\eta,c}(1) \in (0.5, 1)$. The boundary condition sorts out the $\psi^+(\eta)$ component at origin and infinity, and there is no relevant branch cut to cross. One can write down the relation of the wave functions by matrix multiplication

$$\begin{pmatrix} \psi_{a,I_\infty}^+(\eta) \\ \psi_{a,I_\infty}^-(\eta) \end{pmatrix} = M_+^{-1} N_{ab} M_+^{-1} N_{ba} \begin{pmatrix} \psi_{a,I_0}^+(\eta) \\ \psi_{a,I_0}^-(\eta) \end{pmatrix} = \begin{pmatrix} \psi_{a,I_0}^+(\eta) - i(1 + \mathcal{V}_\gamma) \psi_{a,I_0}^-(\eta) \\ \psi_{a,I_0}^-(\eta) \end{pmatrix}, \quad (3.36)$$

for small F and

$$\begin{pmatrix} \psi_{a,I_\infty}^+(\eta) \\ \psi_{a,I_\infty}^-(\eta) \end{pmatrix} = M_+^{-1} N_{ac} M_+^{-1} N_{cb} M_+^{-1} N_{bc} N_{ca} \begin{pmatrix} \psi_{a,I_0}^+(\eta) \\ \psi_{a,I_0}^-(\eta) \end{pmatrix} = \begin{pmatrix} \psi_{a,I_0}^+(\eta) - i(1 + \mathcal{V}_{\gamma_2} + \mathcal{V}_{\gamma_1} \mathcal{V}_{\gamma_2}) \psi_{a,I_0}^-(\eta) \\ \psi_{a,I_0}^-(\eta) \end{pmatrix}, \quad (3.37)$$

for large F from Stokes graphs figure 1(c) and 1(d) respectively. We use M_+^{-1} because of

the clockwise continuation. So the quantization condition can be written as

$$\Pi_\gamma(\hbar) = \oint P_{\text{even}}(\eta) d\eta = 2\pi i \hbar \left(n_\eta + \frac{1}{2} \right), \text{ for small } F \text{ region,} \quad (3.38)$$

$$\Pi_\gamma(\hbar) + \log \left(1 + e^{-\frac{1}{\hbar} \Pi_{\gamma_1}(\hbar)} \right) = 2\pi i \hbar \left(n_\eta + \frac{1}{2} \right), \text{ for large } F \text{ region,} \quad (3.39)$$

where n_η takes values in non-negative integers. The quantum periods are Borel-resummed as well. Similarly, the last term contributes exponentially small, it can be neglected in the semi-classical limit. The continuity of the two EQCs comes from (3.34) by a similar argument.

3.3 Computation and results

Now we utilize the quantization conditions in the last subsection to compute complex resonant frequencies and compare them with the results from the Riccati-Padé method [33] that shows very high precision. We first establish the classical periods in terms of elliptic integrals.

Classical periods Let us parametrize the potential $Q_0(\xi)$ in the ξ -equation as

$$Q_0(\xi) = \frac{u_0 \xi^3 + u_1 \xi^2 + u_2 \xi + u_3}{\xi^2} = \frac{u_0(\xi - a)(\xi - b)(\xi - c)}{\xi^2}, \quad (3.40)$$

where the coefficients in the potential are related to Stark parameters as (3.11). We consider the relevant period corresponding to one-cycle γ which appears in the quantization condition. The integrals for one-cycle γ_1 can be obtained by the rotation of roots $a \rightarrow b$, $b \rightarrow c$ and $c \rightarrow a$. The classical period is

$$\begin{aligned} \Pi_\xi^{(0)} &= 2\sqrt{u_0} \int_b^a \frac{d\xi}{\xi} \sqrt{(\xi - a)(\xi - b)(\xi - c)} \\ &= 4i \sqrt{\frac{u_0}{a - c}} \left(-s\mathbf{K}(k) + t\mathbf{E}(k) + bc\mathbf{\Pi}(\alpha^2, k) \right), \end{aligned} \quad (3.41)$$

where

$$\begin{aligned} s &= \frac{b(c + 2a) + c(a - c)}{3} = \frac{-c^2 + ac + bc + 2ab}{3}, \\ t &= -\frac{(c - a)(a + b + c)}{3}, \quad k^2 = \frac{a - b}{a - c}, \quad \alpha^2 = \frac{a - b}{a}. \end{aligned} \quad (3.42)$$

$\mathbf{K}(k)$, $\mathbf{E}(k)$, and $\mathbf{\Pi}(\alpha^2, k)$ are the elliptic integrals of the first, second, and third kind [38]. The numerical calculation is a bit subtle since the turning points and integral contours are all in the complex coordinate plane, one should be careful about the branch cuts and sheets. Similarly, for the η -equation, we parametrize the potential $Q_0(\eta)$ in (3.12) as

$$Q_0(\eta) = \frac{u_0\eta^3 + u_1\eta^2 + u_2\eta + u_3}{\eta^2} = \frac{u_0(\eta - a)(\eta - b)(\eta - c)}{\eta^2}. \quad (3.43)$$

The classical period is evaluated as

$$\begin{aligned} \Pi_\eta^{(0)} &= 2\sqrt{u_0} \int_a^b \frac{d\eta}{\eta} \sqrt{(\eta - a)(\eta - b)(\eta - c)} \\ &= 4\sqrt{\frac{u_0}{c - a}} \{s\mathbf{K}(k) - t\mathbf{E}(k) - bc\mathbf{\Pi}(\alpha^2, k)\}, \end{aligned} \quad (3.44)$$

here $u_0 = -\frac{F}{4}$ is negative, which gives an overall imaginary unit i . These formulas have already appeared in the literature like [12], but the conventions are different from an imaginary unit i . It is almost impossible to compute quantum period by direct integration, yet there is a systematic method based on the Picard-Fuchs equation to evaluate these quantities. It can be sketched by introducing the following fundamental periods.

Fundamental periods We first define the differential

$$\begin{aligned} \lambda_1 &= \partial_{u_1} \sqrt{Q_0(x)} dx = \frac{1}{2\sqrt{Q_0(x)}} dx, \\ \lambda_2 &= \partial_{u_2} \sqrt{Q_0(x)} dx = \frac{1}{2x\sqrt{Q_0(x)}} dx, \\ \lambda_3 &= \partial_{u_3} \sqrt{Q_0(x)} dx = \frac{1}{2x^2\sqrt{Q_0(x)}} dx. \end{aligned} \quad (3.45)$$

We use x to represent ξ or η uniformly for simplicity. It was found that all $p_{2n}(x)$ can be expressed by the combination of the above fundamental differentials up to a total derivative

$$p_{2n}(x) = \sum_{i=1}^3 c_i^{(n)} \lambda_i + d(*). \quad (3.46)$$

The \hbar expansions for the quantum periods can be evaluated by determining the Picard-Fuchs coefficients $c_i^{(n)}$ and the fundamental periods, which are defined as

$$(\Pi_\xi)_i = \oint_\gamma \lambda_i, \quad i = 1, 2, 3. \quad (3.47)$$

It can be evaluated in terms of elliptic integrals

$$\begin{aligned}
(\Pi_\xi)_1 &= \oint_\gamma \lambda_1 = \int_b^a \frac{d\xi}{\sqrt{Q_0(\xi)}} = \frac{i}{\sqrt{u_0}} \left(\frac{c}{\sqrt{a-c}} \mathbf{K}(k) + \sqrt{a-c} \mathbf{E}(k) \right), \\
(\Pi_\xi)_2 &= \oint_\gamma \lambda_2 = \int_b^a \frac{d\xi}{\xi \sqrt{Q_0(\xi)}} = \frac{i}{\sqrt{u_0}} \frac{1}{\sqrt{a-c}} \mathbf{K}(k), \\
(\Pi_\xi)_3 &= \oint_\gamma \lambda_3 = \int_b^a \frac{d\xi}{\xi^2 \sqrt{Q_0(\xi)}} = \frac{i}{\sqrt{u_0}} \frac{1}{a\sqrt{a-c}} \mathbf{\Pi}(\alpha^2, k).
\end{aligned} \tag{3.48}$$

Similarly, the fundamental periods for η coordinate are evaluated as follows

$$\begin{aligned}
(\Pi_\eta)_1 &= -\frac{1}{\sqrt{u_0}} \left(\frac{c}{\sqrt{c-a}} \mathbf{K}(k) - \sqrt{c-a} \mathbf{E}(k) \right), \\
(\Pi_\eta)_2 &= -\frac{1}{\sqrt{u_0}} \frac{1}{\sqrt{c-a}} \mathbf{K}(k), \quad (\Pi_\eta)_3 = -\frac{1}{\sqrt{u_0}} \frac{1}{a\sqrt{c-a}} \mathbf{\Pi}(\alpha^2, k),
\end{aligned} \tag{3.49}$$

here u_0 is negative as well. Then the quantum periods are given by

$$\Pi_{\xi,\eta}(\hbar) = \sum_{n=0}^{\infty} \hbar^{2n} \left(c_1^{(n)} (\Pi_{\xi,\eta})_1 + c_2^{(n)} (\Pi_{\xi,\eta})_2 + c_3^{(n)} (\Pi_{\xi,\eta})_3 \right), \tag{3.50}$$

where the first several order Picard-Fuchs coefficients are listed as follows

$$\begin{aligned}
c_1^{(0)} &= \frac{2u_1}{3}, \quad c_2^{(0)} = \frac{4u_2}{3}, \quad c_3^{(0)} = 2u_3, \\
c_1^{(1)} &= \frac{u_0 (u_2 (u_1^2 - 6u_0 u_2) + 9u_0 u_1 u_3)}{12 (-18u_0 u_1 u_2 u_3 + u_0 (27u_0 u_3^2 + 4u_2^3) + 4u_1^3 u_3 - u_1^2 u_2^2)}, \\
c_2^{(1)} &= -\frac{u_0 (9u_0 u_2 u_3 - 6u_1^2 u_3 + u_1 u_2^2)}{12 (-18u_0 u_1 u_2 u_3 + u_0 (27u_0 u_3^2 + 4u_2^3) + 4u_1^3 u_3 - u_1^2 u_2^2)}, \quad c_3^{(1)} = 0.
\end{aligned} \tag{3.51}$$

The higher-order coefficients are too long to list here. We use short notations $u_0 = \frac{F}{4}$, $u_1 = -\frac{E}{2}$, $u_2 = -A_1$ and $u_3 = \frac{m^2}{4}$ for the ξ -equation, $u_0 = -\frac{F}{4}$, $u_1 = -\frac{E}{2}$, $u_2 = -(1 - A_1)$ and $u_3 = \frac{m^2}{4}$ for the η -equation here. The computation indicates all $c_3^{(n)} = 0$ for $n > 0$. All these coefficients are independent of 1-cycle from its definition, so they also apply to γ_1 and γ_2 .

Numerical calculations Although we have derived the EQCs in terms of Borel-resummed quantum periods, it is of course impossible to calculate all-orders quantum corrections explicitly. But one can solve the EQCs by accounting for the first several orders of quantum

periods. Since the divergence of all-orders expansions of quantum periods, numerical techniques such as the Borel-Padé method are necessary.

F	0.03	0.1	10
$m = 0$	$-0.500960 - 2.954[13]i$	$-0.511243 - 1.708[7]i$	$0.523489 - 4.70091i$
	$-0.502074 - 1.119[8]i$	$-0.527418 - 0.007269i$	$0.608272 - 5.57802i$
$m = \frac{1}{2}$	$-0.230519 - 0.049799i$	$-0.284888 - 0.086220i$	$1.91824 - 7.77651i$
	$-0.240498 - 0.007357i$	$-0.275297 - 0.099408i$	$2.29507 - 7.89113i$
$m = 1$	$-0.156886 - 0.040912i$	$-0.157828 - 0.197070i$	$3.24392 - 9.75365i$
	$-0.153357 - 0.044424i$	$-0.154012 - 0.201879i$	$3.59267 - 9.82232i$
$m = \frac{3}{2}$	$-0.103499 - 0.084042i$	$-0.071633 - 0.289999i$	$4.35986 - 11.4925i$
	$-0.101927 - 0.085442i$	$-0.070198 - 0.293556i$	$4.69979 - 11.5350i$
$m = 2$	$-0.065022 - 0.122749i$	$-0.003960 - 0.373116i$	$5.35259 - 13.0768i$
	$-0.064236 - 0.123769i$	$-0.003500 - 0.376159i$	$5.68990 - 13.1015i$
$m = \frac{5}{2}$	$-0.034074 - 0.158318i$	$0.053480 - 0.449186i$	$6.26167 - 14.5494i$
	$-0.033645 - 0.159169i$	$0.053447 - 0.451947i$	$6.59891 - 14.5609i$
$m = 3$	$-0.007590 - 0.191362i$	$0.104377 - 0.519926i$	$7.10904 - 15.9364i$
	$-0.007353 - 0.192112i$	$0.104058 - 0.522512i$	$7.44738 - 15.9374i$

Table 3.1: The table shows complex resonant frequencies E for distinct magnetic quantum number m with electric field strength from weak to very strong. The first row stands for the results computed from quantization conditions (3.29) and (3.38) for $F = 0.03, 0.1$, and conditions (3.33) and (3.39) for $F = 10$. Here only classical periods $\Pi^{(0)}$ are considered. And the second row is for the Riccati-Padé method. [a] means 10^{-a} , this notation is also used later.

It is straightforward to calculate the complex energy by simultaneously solving quantization conditions for ξ - and η -equations. We show the numerical result for $F = 0.03, 0.1, 10$

and m from 0 to 3 with half unit in table 3.1. For the $m = 0$ case, the turning point b collapses to 0, and the elliptic integral of third kind $\mathbf{\Pi}(\alpha^2, k)$ becomes zero. We adopt BS quantization conditions (3.29) and (3.38) for $F = 0.03$ and $F = 0.1$ and modified BS quantization conditions (3.33) and (3.39) for $F = 10$. At this stage, we only consider the first-order contribution, namely $\mathbf{\Pi}^{(0)}$. For convenience to compare with other methods, both quantum numbers n_ξ and n_η are set to 0. In fact, it is the worst case for the application of the WKB method, since it approximates much better for large n states. We find even the first-order WKB analysis gives good estimation for a wide range of parameter choices. As a matter of fact, $F = 0.03$ is already a strong field intensity in the atomic unit. If one examines for very weak field F , the result shows high precision as in [12]. The calculation indicates even for a very strong field, for example, $F = 10$ here, the approximation is also efficient.

We also find the effect of the logarithmic term in modified BS quantization conditions (3.33) and (3.39). Table 3.2 shows the complex energies for a strong field intensity $F = 5$ and $m = 1, 2, 3$, which belong to the strong F region for both ξ - and η -equations. It is obvious that quantization conditions including the logarithmic term give closer results to exact values. Our observation further implies the imaginary part gets corrected significantly by the additional modified term.

$F = 5$	$m = 1$	$m = 2$	$m = 3$
1st-order BSQC	$2.32739 - 7.03055i$	$3.54168 - 9.13333i$	$4.58412 - 10.9252i$
1st-order EQC	$1.70365 - 5.72785i$	$3.08635 - 7.85116i$	$4.22348 - 9.67094i$
RPM	$1.87776 - 5.82185i$	$3.24425 - 7.91809i$	$4.37684 - 9.72372i$

Table 3.2: This shows the complex resonant frequencies for $F = 5$ and $m = 1, 2$ and 3. The first and second row represents the results from BS quantization conditions and modified quantization condition including the additional logarithm correction respectively. Here only contributions from classical periods $\mathbf{\Pi}^{(0)}$ are included.

One of the new results in this paper is to include the quantum corrections to $\Pi^{(0)}$. Table 3.3 exhibits the results for $F = 0.005$ by including the first several orders of quantum periods. The energy level for the ground state is really precise, the imaginary part of complex energy for this case is very small³ and neglected here. However, the improvement for $m = 3$ is not so satisfactory. One quick reason may be that the quantum corrections are very large compared with classical periods for this case, where the numerical approximation performs not well even the Borel-Padé technique is adopted.

azimuthal number(m)	0	3
$\mathcal{O}(\hbar^0)$	-0.5000265658500433	-0.0402674 - 0.0326842 <i>i</i>
$\mathcal{O}(\hbar^2)$	-0.5000562669655335	-0.0401851 - 0.0327634 <i>i</i>
$\mathcal{O}(\hbar^4)$	-0.5000562847698887	-0.0401867 - 0.0327546 <i>i</i>
$\mathcal{O}(\hbar^6)$	-0.5000562847937314	-0.0401877 - 0.0327561 <i>i</i>
$\mathcal{O}(\hbar^8)$	-0.5000562847937927	-0.0401869 - 0.0327561 <i>i</i>
RPM	-0.5000562847937930	-0.0400286 - 0.0328640 <i>i</i>

Table 3.3: Complex energy frequencies for electric field strength $F = 0.005$ with azimuthal quantum number $m = 0$ and $m = 3$ respectively.

It is not expected in general that the present method entirely matches with standard perturbation theory results for each order of \hbar except for the first order. Since our method is based on Langer's modification which is just a kind of expansion scheme. Different schemes give different results, but they all coincide to include all-orders \hbar expansions. In practice, we use the first several leading orders to approximate the exact Borel-resummed quantum WKB periods as a numerical approach.

³approximately 10^{-56} as shown in [39]

4 TBA equations and analytic continuation

The quantum period is the fundamental ingredient in the WKB analysis, however, it can be established from another approach based on the ODE/IM correspondence. Since Langer's modification is not necessary for this analysis, we will not consider the modification in this section. But both setups are the same when $m = 0$.

4.1 Singular potentials and quantum periods

Let us now revisit the Stark problem without Langer's modification to reconsider (3.4), which is uniformly written as (3.5). We will consider quantum periods from WKB expansions at first. We use the same notations for $Q_0(x)$, $\Pi(\hbar)$, and γ which should not be confused with the prescription adopted in the last section. The classical and quantum periods can be written in terms of elliptic integrals.

Classical periods Denote two turning points e_1 and e_2 of $Q_0(x)$ in (3.5):

$$Q_0(x) = \frac{u_0x^2 + u_1x + u_2}{x} = \frac{u_0(x - e_1)(x - e_2)}{x}, \quad e_{1,2} = \frac{-u_1 \pm \sqrt{u_1^2 - 4u_0u_2}}{2u_0}. \quad (4.1)$$

One can define three one-cycles on the Riemann surface defined by $y^2 = Q_0(x)$, which encircle e_1 and e_2 , 0 and e_1 , 0 and e_2 and are denoted as γ , $\hat{\gamma}_1$ and $\hat{\gamma}_2$ respectively. Then the classical periods corresponding to these three cycles are represented by the elliptic integrals as

$$\begin{aligned} \Pi_\gamma^{(0)} &= 2 \int_{e_1}^{e_2} \sqrt{Q_0(x)} dx = 2i(e_2 - e_1)^2 \sqrt{\frac{u_0}{e_1}} \frac{4(2+k)\mathbf{E}(-k) - 8(1+k)\mathbf{K}(-k)}{6k^2}, \\ \Pi_{\hat{\gamma}_1}^{(0)} &= 2 \int_0^{e_1} \sqrt{Q_0(x)} dx = \frac{4}{3} \sqrt{u_0 e_1^3 m} \left((1+m)\mathbf{E}\left(\frac{1}{m}\right) - (m-1)\mathbf{K}\left(\frac{1}{m}\right) \right), \\ \Pi_{\hat{\gamma}_2}^{(0)} &= 2 \int_{e_2}^0 \sqrt{Q_0(x)} dx = -\frac{4}{3} \sqrt{\frac{u_0 e_2^3}{m}} \left(\left(1 + \frac{1}{m}\right)\mathbf{E}(m) - \left(\frac{1}{m} - 1\right)\mathbf{K}(m) \right), \end{aligned} \quad (4.2)$$

where $m = \frac{e_2}{e_1}$ and $k = \frac{e_2}{e_1} - 1$. These periods are related by their definitions

$$\Pi_\gamma^{(0)} + \Pi_{\hat{\gamma}_1}^{(0)} + \Pi_{\hat{\gamma}_2}^{(0)} = 0. \quad (4.3)$$

The quantum periods are evaluated by the Picard-Fuchs method as well, which is composed of a combination of fundamental periods.

Fundamental periods Define the fundamental differentials first for $Q_0(x)$:

$$\begin{aligned}\lambda_1 &= \partial_{u_1} \sqrt{Q_0(x)} dx = \frac{1}{2\sqrt{Q_0(x)}} dx, \\ \lambda_2 &= \partial_{u_2} \sqrt{Q_0(x)} dx = \frac{1}{2x\sqrt{Q_0(x)}} dx,\end{aligned}\tag{4.4}$$

and the associated fundamental periods

$$(\Pi_\gamma)_i = \oint_\gamma \lambda_i.\tag{4.5}$$

They are represented as

$$(\Pi_\gamma)_1 = \int_{e_1}^{e_2} \frac{dx}{\sqrt{Q_0(x)}} = -2i\sqrt{\frac{e_1}{u_0}} \mathbf{E}(-k), \quad (\Pi_\gamma)_2 = \int_{e_1}^{e_2} \frac{dx}{x\sqrt{Q_0(x)}} = -\frac{2i}{\sqrt{u_0 e_1}} \mathbf{K}(-k),\tag{4.6}$$

$$(\Pi_{\hat{\gamma}_1})_1 = \int_0^{e_1} \frac{dx}{\sqrt{Q_0(x)}} = 2\sqrt{\frac{u_0 m e_1^3}{u_1^2}} \left((1+m)\mathbf{E}\left(\frac{1}{m}\right) - (m-1)\mathbf{K}\left(\frac{1}{m}\right) \right) - \frac{u_2}{u_1} \frac{4}{\sqrt{u_0 e_1 m}} \mathbf{K}\left(\frac{1}{m}\right),\tag{4.7}$$

$$(\Pi_{\hat{\gamma}_1})_2 = \int_0^{e_1} \frac{dx}{x\sqrt{Q_0(x)}} = \frac{2}{\sqrt{u_0 e_1 m}} \mathbf{K}\left(\frac{1}{m}\right),\tag{4.8}$$

$$(\Pi_{\hat{\gamma}_2})_1 = \int_{e_2}^0 \frac{dx}{\sqrt{Q_0(x)}} = \frac{4u_2}{u_1} \sqrt{\frac{m}{u_0 e_2}} \mathbf{K}(m) - 2\sqrt{\frac{u_0 e_2^3}{m u_1^2}} \left(\left(1 + \frac{1}{m}\right)\mathbf{E}(m) - \left(\frac{1}{m} - 1\right)\mathbf{K}(m) \right),\tag{4.9}$$

$$(\Pi_{\hat{\gamma}_2})_2 = \int_{e_2}^0 \frac{dx}{x\sqrt{Q_0(x)}} = -2\sqrt{\frac{m}{u_0 e_2}} \mathbf{K}(m).\tag{4.10}$$

As the same as (3.46), there is a similar relation

$$p_{2n}(x) = \sum_{i=1}^2 c_i^{(n)} \lambda_i + d(*),\tag{4.11}$$

which suggests writing down quantum periods by

$$\Pi(\hbar) = \sum_{n=0}^{\infty} \hbar^{2n} \left(c_1^{(n)}(\Pi)_1 + c_2^{(n)}(\Pi)_2 \right), \quad (4.12)$$

where the subscript $\gamma, \hat{\gamma}_1$, and $\hat{\gamma}_2$ are omitted. The Picard-Fuchs coefficients $c_{1,2}^{(n)}$ can be obtained similarly as (3.51), they are of course different although we abuse the same notations. The first several coefficients are listed as follows

$$\begin{aligned} c_1^{(0)} &= \frac{2u_1}{3}, & c_2^{(0)} &= \frac{4u_2}{3}, \\ c_1^{(1)} &= \frac{1}{6}u_0 \left(\frac{6\ell(\ell+1)+1}{u_2} + \frac{u_0}{u_1^2 - 4u_0u_2} \right), & c_2^{(1)} &= \frac{u_0u_1}{12(u_1^2 - 4u_0u_2)}, \end{aligned} \quad (4.13)$$

where ℓ is related to m by (3.7).

4.2 TBA equations for the minimal chamber

Now we study the quantum period with its relation to the TBA equations. Let us consider

$$\left(-\hbar^2 \frac{d^2}{dx^2} + u_0x + u_1 + \frac{u_2}{x} + \frac{\hbar^2 \ell(\ell+1)}{x^2} \right) \psi(x) = 0. \quad (4.14)$$

The TBA equations for (4.14) within $-1 < \ell < 1$ were first proposed in [31].

$$\begin{aligned} \log Y_1(\theta) &= -m_1 e^\theta + \int_{-\infty}^{\infty} \frac{d\theta'}{2\pi} \frac{\log \left(1 - e^{2\pi i \ell} \hat{Y}(\theta') \right) \left(1 - e^{-2\pi i \ell} \hat{Y}(\theta') \right)}{\cosh(\theta - \theta')}, \\ \log \hat{Y}(\theta) &= -\hat{m} e^\theta + \int_{-\infty}^{\infty} \frac{d\theta'}{2\pi} \frac{\log(1 + Y_1(\theta'))}{\cosh(\theta - \theta')}. \end{aligned} \quad (4.15)$$

Here $-\log Y_1(\theta)$ and $-\log \hat{Y}(\theta)$ correspond to the energies of the pseudo-particles in the integrable system. A new parameter $\theta = -\log \hbar$ called the rapidity is introduced, which takes the semi-classical limit $\hbar \rightarrow 0$ to $\theta \rightarrow \infty$. The large θ expansion of the Y functions is captured by the classical period

$$\begin{aligned} Y_1(\theta) &\sim e^{-\frac{m_1}{\hbar}}, & m_1 &\equiv -i \oint_{\gamma} \sqrt{Q_0(x)} dx = -i \Pi_{\gamma}^{(0)}, \\ \hat{Y}(\theta) &\sim e^{-\frac{\hat{m}}{\hbar}}, & \hat{m} &\equiv \oint_{\hat{\gamma}_1} \sqrt{Q_0(x)} dx = \Pi_{\hat{\gamma}_1}^{(0)}. \end{aligned} \quad (4.16)$$

Moreover, the higher-order expansions of the Y function for large θ are consistent with all-order quantum periods. When the mass parameters m_1 and \hat{m} are complex, we set

$$m_1 = |m_1| e^{i\phi_1}, \quad \hat{m} = |\hat{m}| e^{i\hat{\phi}}, \quad (4.17)$$

then the driving term in (4.15) becomes $m_1 e^\theta = |m_1| e^{\theta+i\phi_1}$ and $\hat{m} e^\theta = |\hat{m}| e^{\theta+i\hat{\phi}}$. We shift $\theta \rightarrow \theta - i\phi_1$ for $Y_1(\theta)$ and $\theta \rightarrow \theta - i\hat{\phi}$ for $\hat{Y}(\theta)$ so that the TBA equations becomes

$$\begin{aligned} \log Y_1(\theta - i\phi_1) &= -|m_1| e^\theta + \int_{-\infty}^{\infty} \frac{d\theta'}{2\pi} \frac{\log \left(1 - e^{2\pi i l \hat{Y}(\theta' - i\hat{\phi})} \right) \left(1 - e^{-2\pi i l \hat{Y}(\theta' - i\hat{\phi})} \right)}{\cosh \left(\theta - \theta' - i\phi_1 + i\hat{\phi} \right)}, \\ \log \hat{Y}(\theta - i\hat{\phi}) &= -|\hat{m}| e^\theta + \int_{-\infty}^{\infty} \frac{d\theta'}{2\pi} \frac{\log(1 + Y_1(\theta - i\phi_1))}{\cosh \left(\theta - \theta' - i\hat{\phi} + i\phi_1 \right)}. \end{aligned} \quad (4.18)$$

These equations hold when

$$|\phi_1 - \hat{\phi}| < \frac{\pi}{2}, \quad (4.19)$$

which defines a region in the space of parameters u_0 , u_1 , and u_2 . It is called the minimal chamber. If we rotate \hbar to redefine a new constant $\tilde{\hbar} = i\hbar$, then the equation for η coordinate becomes

$$\left(-\tilde{\hbar}^2 \frac{d^2}{d\eta^2} + \frac{F}{4}\eta + \frac{E}{2} + \frac{A_2}{\eta} + \frac{\tilde{\hbar}^2(m^2 - 1)}{4\eta^2} \right) \psi_2(\eta) = 0. \quad (4.20)$$

We found the parameters for the ground state with $m = 0$ lie in the minimal chamber now. We solve these TBA equations iteratively via the Fourier discretization by taking m_1 and \hat{m} as the initial seed and compute the first several order expansions by the large θ expansion for $\log Y(\theta)$

$$\begin{aligned} -\log Y_1(\theta) &\sim m_1 e^\theta + \sum_{n \geq 1} m_1^{(n)} e^{(1-2n)\theta}, \\ -\log \hat{Y}(\theta) &\sim \hat{m} e^\theta + \sum_{n \geq 1} \hat{m}^{(n)} e^{(1-2n)\theta}. \end{aligned} \quad (4.21)$$

The expansion coefficients are

$$\begin{aligned} m_1^{(n)} &= \frac{(-1)^n}{\pi} \int_{\mathbb{R}} e^{(2n-1)\theta'} \left[\log \left(1 - e^{2\pi i l \hat{Y}}(\theta') \right) + \log \left(1 - e^{-2\pi i l \hat{Y}}(\theta') \right) \right] d\theta', \\ \hat{m}^{(n)} &= \frac{(-1)^n}{\pi} \int_{\mathbb{R}} e^{(2n-1)\theta'} \log \left(1 + Y_1(\theta') \right) d\theta', \end{aligned} \quad (4.22)$$

here we suppose m_1 and \hat{m} are real. The ODE/IM correspondence implies the following relationship

$$im_1^{(n)} = (-1)^n \Pi_{\gamma}^{(n)}, \quad \hat{m}^{(n)} = \Pi_{\hat{\gamma}_1}^{(n)}, \quad (4.23)$$

where $m_1^{(0)} = m_1$ and $\hat{m}^{(0)} = \hat{m}$ are mass parameters. Numeric results are listed in table 4.1 for $\ell = -\frac{1}{2}$ or $m = 0$ and $F = 0.005$, where E and A_1 are substituted as input parameters. We utilize the precise value of E in table 3.1 and A_1 from the Riccati-Padé method to compute the classical period $\Pi^{(0)}$, which equivalently gives mass parameters m and \hat{m} . Large θ expansions $m^{(n)}$ are compared with the quantum periods $\Pi^{(n)}$ calculated by the Picard-Fuchs method for the first several orders to find them in good agreement.

n	$m_1^{(n)}$	$\hat{m}^{(n)}$	$\Pi_{\gamma}^{(n)}$	$\Pi_{\hat{\gamma}_1}^{(n)}$
1	-0.17229336876340	-0.00405302352020	0.17229336876307i	-0.00405302352018
2	0.03925568525637	6.009535667649[7]	0.03925568525630i	6.009535667620[7]
3	-0.04967657873047	-4.680585382632[10]	0.04967657873075i	-4.680585382628[10]

Table 4.1: First three order expansions of the quantum periods for η -equation from TBA equations and Picard-Fuchs method for $m = 0$ and $F = 0.005$.

Continuation of ℓ The authors in [35] found as ℓ goes from $-1 < \ell < 0$ to $\ell > 0$, TBA equations get modified from the singularities of the Y equations in the complex θ plane [34]. When $0 < \ell \lesssim 0.28$, which is named the first modified region in [35], the TBA

equations are

$$\begin{aligned}\log Y_1(\theta) &= -m_1 e^\theta + \int_{\mathbb{R}} \frac{d\theta'}{2\pi} \frac{\log \left(\left(1 - e^{2\pi i \ell} \hat{Y}(\theta')\right) \left(1 - e^{-2\pi i \ell} \hat{Y}(\theta')\right) \right)}{\cosh(\theta - \theta')} + \log \left(\frac{e^\theta + i e^{\alpha_1(\ell)}}{e^\theta - i e^{\alpha_1(\ell)}} \right), \\ \log \hat{Y}(\theta) &= -\hat{m} e^\theta + \int_{\mathbb{R}} \frac{d\theta'}{2\pi} \frac{\log(1 + Y_1(\theta'))}{\cosh(\theta - \theta')},\end{aligned}\tag{4.24}$$

where $\alpha_1(\ell)$ is the zero of $1 - e^{2\pi i \ell} \hat{Y}(\theta)$ in the $|\text{Im}(\theta)| < \frac{\pi}{2}$ strip, and is determined by

$$2\pi i \ell = -\log \hat{Y}(\alpha_1(\ell)) = \hat{m} e^{\alpha_1(\ell)} - \int_{\mathbb{R}} \frac{d\theta'}{2\pi} \frac{\log(1 + Y_1(\theta'))}{\cosh(\alpha_1(\ell) - \theta')}.\tag{4.25}$$

The algorithm for solving these TBA equations refers to [35]. In this case, expansions of the quantum periods are also modified by $\alpha_1(\ell)$.

$$\begin{aligned}m_1^{(n)} &= (-1)^n \left(\frac{1}{\pi} \int_{\mathbb{R}} e^{(2n-1)\theta'} \left\{ \log \left(1 - e^{2\pi i \ell} \hat{Y}(\theta') \right) + \log \left(1 - e^{-2\pi i \ell} \hat{Y}(\theta') \right) \right\} d\theta' + 2i \frac{e^{(2n-1)\alpha_1(\ell)}}{2n-1} \right), \\ \hat{m}^{(n)} &= \frac{(-1)^n}{\pi} \int_{\mathbb{R}} e^{(2n-1)\theta'} \log(1 + Y_1(\theta')) d\theta'.\end{aligned}\tag{4.26}$$

However, it seems the parameters u_0, u_1 , and u_2 for $\ell > 0$ are already outside the minimal chamber. But we can test the relationship (4.23) for some fictitious value, $u_0 = 1, u_1 = -3, u_2 = 1$ and $\ell = \frac{1}{5}$ to confirm this correspondence holds on with ℓ correction. This is not covered in [35]. We list the numeric results in table 4.2 to compare with those evaluated from the Picard-Fuchs method. See also [40] for further discussions.

n	$m_1^{(n)}$	$\hat{m}^{(n)}$	$\Pi_\gamma^{(n)}$	$\Pi_{\hat{\gamma}_1}^{(n)}$
1	1.4753093535348	0.0720517742848	$-1.4753093522562i$	0.0720517728119
2	0.2019237645206	0.0000700313547	$0.2019237643494i$	0.0000700315059
3	0.2508765451711	-0.0045008552377	$-0.2508765449614i$	-0.0045008554033
4	-1.4745761911756	0.0180119220334	$-1.4745761905853i$	0.0180119208494

Table 4.2: First four order expansions of the quantum periods for fictitious parameters $u_0 = 1, u_1 = -3, u_2 = 1$ and $\ell = \frac{1}{5}$.

As ℓ increases steadily, the second singular point for the Y function gets involved, and the ℓ enters into the second modified region $0.28 \lesssim \ell \lesssim 0.5$. The TBA equations for this region are

$$\begin{aligned}\log Y_1(\theta) &= -m_1 e^\theta + \int_{\mathbb{R}} \frac{d\theta'}{2\pi} \frac{\log \left(\left(1 - e^{2\pi i \ell} \hat{Y}(\theta')\right) \left(1 - e^{-2\pi i \ell} \hat{Y}(\theta')\right) \right)}{\cosh(\theta - \theta')} + \log \left(\frac{e^\theta + i e^{\alpha_1(\ell)}}{e^\theta - i e^{\alpha_1(\ell)}} \right), \\ \log \hat{Y}(\theta) &= -\hat{m} e^\theta + \int_{\mathbb{R}} \frac{d\theta'}{2\pi} \frac{\log(1 + Y_1(\theta'))}{\cosh(\theta - \theta')} + \log \left(\frac{e^\theta + i e^{\hat{\alpha}(\ell)}}{e^\theta - i e^{\hat{\alpha}(\ell)}} \right),\end{aligned}\tag{4.27}$$

where $\alpha_1(\ell)$ and $\hat{\alpha}(\ell)$ are determined by

$$\begin{aligned}2\pi i \ell &= \hat{m} e^{\alpha_1(\ell)} - \int_{\mathbb{R}} \frac{\log(1 + Y_1(\theta'))}{\cosh(\alpha_1(\ell) - \theta')} \frac{d\theta'}{2\pi} - \log \left(\frac{e^{\alpha_1(\ell)} + i e^{\hat{\alpha}(\ell)}}{e^{\alpha_1(\ell)} - i e^{\hat{\alpha}(\ell)}} \right) \\ -\pi i &= m_1 e^{\hat{\alpha}(\ell)} - \int_{\mathbb{R}} \frac{\log \left(\left(1 - e^{2\pi i \ell} \hat{Y}(\theta')\right) \left(1 - e^{-2\pi i \ell} \hat{Y}(\theta')\right) \right)}{\cosh(\hat{\alpha}(\ell) - \theta')} \frac{d\theta'}{2\pi} - \log \left(\frac{e^{\hat{\alpha}(\ell)} + i e^{\alpha_1(\ell)}}{e^{\hat{\alpha}(\ell)} - i e^{\alpha_1(\ell)}} \right).\end{aligned}\tag{4.28}$$

In this case, quantum periods are modified by $\alpha_1(\ell)$ and $\hat{\alpha}(\ell)$ as follows

$$\begin{aligned}m_1^{(n)} &= \frac{(-1)^n}{\pi} \left(\int_{\mathbb{R}} e^{(2n-1)\theta'} \left\{ \log \left(1 - e^{2\pi i \ell} \hat{Y}(\theta')\right) + \log \left(1 - e^{-2\pi i \ell} \hat{Y}(\theta')\right) \right\} d\theta' + 2i \frac{e^{(2n-1)\alpha_1(\ell)}}{2n-1} \right) \\ \hat{m}^{(n)} &= \frac{(-1)^n}{\pi} \left(\int_{\mathbb{R}} e^{(2n-1)\theta'} \log(1 + Y_1(\theta')) d\theta' + 2i \frac{e^{(2n-1)\hat{\alpha}(\ell)}}{2n-1} \right)\end{aligned}\tag{4.29}$$

n	$m_1^{(n)}$	$\hat{m}^{(n)}$	$\Pi_\gamma^{(n)}$	$\Pi_{\hat{\gamma}_1}^{(n)}$
1	2.6562188814454	0.1978678217639	$-2.6562188791176i$	0.19786781876613
2	1.9329727067243	-0.0054720259650	$1.9329727050823i$	-0.00547202448659
3	1.6659668485245	0.0005791023097	$-1.6659668471070i$	0.00057910105643
4	6.7514239599655	0.0064465654840	$6.7514239558741i$	0.00644657053159

Table 4.3: Quantum periods for $u_0 = 1, u_1 = -3, u_2 = 1$ and $\ell = \frac{2}{5}$.

Table 4.3 shows the first four expansions of the quantum periods computed from the

above expansions and the Picard-Fuchs method. We also adopt unphysical moduli parameters $u_0 = 1, u_1 = -3, u_2 = 1$, and $\ell = \frac{2}{5}$. They are all consistent for the given precision.

One can find that the quantum periods calculated directly from the Picard-Fuchs method agree well with the evaluation from the TBA side for wide parameter choices, which verifies the generalized ODE/IM correspondence.

4.3 Analytic continuation and wall-crossing

The TBA equations (4.18) are valid only when (4.19) is satisfied. The kernel function

$$\frac{1}{\cosh\left(\theta - \theta' - i\phi_1 + i\hat{\phi}\right)} \quad (4.30)$$

has poles at

$$\theta' = \theta - i\phi_1 + i\hat{\phi} + \frac{i\pi}{2} + in\pi, \quad n \in \mathbb{Z}, \quad (4.31)$$

where $\theta - i\phi_1 + i\hat{\phi} - \frac{i\pi}{2}$ locates below the real axis and $\theta - i\phi_1 + i\hat{\phi} + \frac{i\pi}{2}$ above the real axis. When $\phi_1 - \hat{\phi}$ increases and cross over $\phi_1 - \hat{\phi} > \frac{\pi}{2}$, the pole $\theta - i\phi_1 + i\hat{\phi} + \frac{i\pi}{2}$ moves down and cross the real axis. The θ' -integral picks the residue at this pole. Similarly the second equation in (4.18) picks the pole at $\theta - i\phi_1 + i\hat{\phi} - \frac{i\pi}{2}$. This phenomenon is the wall-crossing of the TBA equations. The TBA equations after wall-crossing are modified as Appendix B in [31].

We found the situation simplifies for a special choice of ℓ , where the quantum periods follow compact TBA equations for quartic double-well potentials. Firstly, one notes under the coordinate transformation $x \rightarrow z^2$ and function rescale $\psi(x) \rightarrow z^{\frac{1}{2}}\phi(z)$, the original equation (4.14) becomes

$$\left(-\hbar^2 \frac{d^2}{dz^2} + (4u_0z^4 + 4u_1z^2 + 4u_2) + \hbar^2 \frac{16\ell(\ell+1)+3}{4z^2}\right) \phi(z) = 0. \quad (4.32)$$

For $\ell = -\frac{1}{4}, -\frac{3}{4}$, or equivalently $m = \frac{1}{2}$, the centrifugal term vanishes. The original equation is mapped to one with a double-well potential, whose TBA equations are already established, for example in [29, 30]. We denote the quantum periods related to (4.14) as

$\Pi_{s,1}^{(n)}$ for one-cycle γ and $\hat{\Pi}_s^{(n)}$ for one-cycle $\hat{\gamma}_1$ defined at the beginning of this section. Quantum periods related to (4.32) are denoted as $\Pi_{q,1}^{(n)}$ and $\hat{\Pi}_q^{(n)}$ for corresponding cycles.

n	$m_1^{(n)}$	$\hat{m}^{(n)}$
0	$4.3446402338816 + 15.4257466346279i$	$-0.0012584924834 - 9.4789003437673i$
1	$0.0266639256955 - 0.0235576487819i$	$0.0012417895471 + 0.0537580797986i$
2	$-1.62952996522[4] - 4.09974572924[4]i$	$1.7792731990[5] + 3.62538591473[4]i$
n	$\Pi_{s,1}^{(n)}$	$2\hat{\Pi}_s^{(n)}$
0	$4.3446402284715i - 15.4257465764022$	$-0.0012584915174 - 9.4789004189858i$
1	$-0.0266639257692i - 0.0235576485732$	$0.0012417895565 + 0.0537580805588i$
2	$-1.62952996537[4]i + 4.09974571511[4]$	$1.77927321993[5] + 3.62538594870[4]i$
n	$\Pi_{q,1}^{(n)}$	$\hat{\Pi}_q^{(n)}$
0	$4.3446402030184 + 15.4257466285002i$	$-0.0012585520475i + 9.4789002636561$
1	$0.0266639255426 - 0.0235576487255i$	$-0.0012417898853i + 0.0537580793133$
2	$-1.62952995392[4] - 4.09974572875[4]i$	$1.77927341291[5]i - 3.62538588259[4]$

Table 4.4: The first two order quantum periods with $F = 0.03$, $m = \frac{1}{2}$ for ξ equation.

We consider a specific case $F = 0.03$ with $m = \frac{1}{2}$. The turning points for (4.32) are $\pm\sqrt{e_1}$ and $\pm\sqrt{e_2}$ with $e_{1,2}$ the turning points for (4.14). Then the classical periods are defined as

$$\begin{aligned}
\Pi_{q,1}^{(0)} &= 2 \int_{-\sqrt{e_1}}^{-\sqrt{e_2}} \sqrt{Q_0^q(x)} dx, & \hat{\Pi}_q^{(0)} &= 2 \int_{-\sqrt{e_1}}^{\sqrt{e_1}} \sqrt{Q_0^q(x)} dx, \text{ for } \xi \text{ variable,} \\
\Pi_{q,1}^{(0)} &= 2 \int_{-\sqrt{e_2}}^{-\sqrt{e_1}} \sqrt{Q_0^q(x)} dx, & \hat{\Pi}_q^{(0)} &= 2 \int_{\sqrt{e_1}}^{-\sqrt{e_1}} \sqrt{Q_0^q(x)} dx, \text{ for } \eta \text{ variable,}
\end{aligned} \tag{4.33}$$

here $Q_0^q(x) = 4u_0z^4 + 4u_1z^2 + 4u_2$ is the quartic potential. The higher orders can be evaluated from the Picard-Fuchs method as well. let us now consider the TBA equations for (4.32). For parameters in η variable, the corresponding TBA equations are in the

minimal chamber as

$$\begin{aligned}\log Y_1(\theta) &= -m_1 e^\theta + \int_{\mathbb{R}} \frac{\log(1 + \hat{Y}(\theta'))}{\cosh(\theta - \theta')} \frac{d\theta'}{2\pi}, \\ \log \hat{Y}(\theta) &= -\hat{m} e^\theta + 2 \int_{\mathbb{R}} \frac{\log(1 + Y_1(\theta'))}{\cosh(\theta - \theta')} \frac{d\theta'}{2\pi}.\end{aligned}\tag{4.34}$$

The TBA equations for the ξ variable are now in the maximal chamber. Equation (5.21) in [29] gives the explicit form of these equations, the mass parameters are related by $m_2 = \hat{m}$, $m_{12} = m_1 - i\hat{m}$, and $m_{123} = 2m_1 - i\hat{m}$ while m_1 is the same as we used in this paper. Then we found the quantum periods and the large θ expansion of the quartic TBA equations are related as follows

$$\begin{aligned}\Pi_{q,1}^{(n)} &= (-1)^{n+1} i \Pi_{s,1}^{(n)} = m_1^{(n)}, & (-1)^{n+1} i \hat{\Pi}_q^{(n)} &= 2\hat{\Pi}_s^{(n)} = \hat{m}^{(n)}, \text{ for } \xi\text{-equation,} \\ \Pi_{q,1}^{(n)} &= (-1)^{n+1} i \Pi_{s,1}^{(n)} = m_1^{(n)}, & (-1)^n i \hat{\Pi}_q^{(n)} &= 2\hat{\Pi}_s^{(n)} = (-1)^n \hat{m}^{(n)}, \text{ for } \eta\text{-equation.}\end{aligned}\tag{4.35}$$

n	$m_1^{(n)}$	$\hat{m}^{(n)}$
0	0.4640679572901 - 0.6555218319259 <i>i</i>	-0.4550034327887 - 8.8968672576106 <i>i</i>
1	0.0007954104344 - 0.054482181983 <i>i</i>	0.3863907823625 + 0.5839673005070 <i>i</i>
2	0.0001177964828 - 0.0015026546306 <i>i</i>	-2.2800851644720 + 0.6221615219336 <i>i</i>
n	$\Pi_{s,1}^{(n)}$	$2\hat{\Pi}_s^{(n)}$
0	0.4640679650555 <i>i</i> + 0.6555217872253	-0.4550034419775 - 8.8968672279807 <i>i</i>
1	-0.0007954088972 <i>i</i> - 0.0544821836255	-0.3863907817713 - 0.5839672972422 <i>i</i>
2	0.0001178053284 <i>i</i> + 0.0015026585094	-2.2800851547326 + 0.6221615231299 <i>i</i>
n	$\Pi_{q,1}^{(n)}$	$\hat{\Pi}_q^{(n)}$
0	0.4640679052528 - 0.6555218495485 <i>i</i>	0.4550034203263 <i>i</i> - 8.8968672224660
1	0.0007954117778 - 0.0544821822247 <i>i</i>	-0.3863907794426 <i>i</i> + 0.5839672977885
2	0.0001177955168 - 0.0015026454486 <i>i</i>	2.2800851542317 <i>i</i> + 0.6221615160777

Table 4.5: The first two order expansions of the quantum periods with $F = 0.03$, $m = \frac{1}{2}$ for η -equation.

Table 4.4 shows the numerical calculations for ξ -equation with $F = 0.03$ and $m = \frac{1}{2}$, where corresponding TBA equations are in the maximal chamber, and table 4.5 gives results for η -equation, with its TBA equations (4.34) in the minimal chamber. Numerical calculations confirm the correspondence (4.35) very well.

In this section, we consider TBA equations related to the Stark problem without Langer's modification. These equations on the one hand confirm the validity of ODE/IM correspondence and give an alternative computational approach for quantum periods on the other hand. Unfortunately, we have not found consistent EQCs in terms of these quantum periods without Langer's modification.

5 Discussion and conclusion

In this paper, we have applied the exact WKB analysis to the well-known Stark problem to resolve the energy frequency and ionization rate simultaneously. This method has several advantages.

- At first, it gives the complex resonant frequency including E_c and ionization rate at the same time, and it applies to a wide range of parameter choices for F and m .
- Second, the analysis is exact as the term EWKB implies, we have derived the exact quantization conditions by utilizing Stokes graphs and found the BS quantization condition is already exact in weak field strength, which clarifies the validity of the WKB approximation and quantization conditions in [11, 12, 13].
- Third, the method presented in this paper is fully analytic in principle, except for the final numerical calculation, which makes it possible to investigate the asymptotic behavior in the limit of the parameters.
- At last, this method can be systematically extended to higher orders, which is crucial to know the large-order behavior of the asymptotic expansions of the quantum periods even its non-perturbative contributions.

We have examined our formulation by numerical calculations which are compared with the results by the Riccati-Padé method in [33] to find agreements. It is proved that this method including Langer's modification and quantum corrections gives a complete resolution of the Stark problem.

In addition, we have discussed the TBA systems related to the Stark problem in the absence of Langer's modification. It gives much more information on the quantum periods by the ODE/IM correspondence. We confirmed the corrections introduced in [35] by comparing the expansions of the logarithm of the Y functions with quantum periods computed from the Picard-Fuchs method. We also discussed the wall-crossing of the TBA equations during the parameters change and wrote down the corresponding quartic TBA equations for special ℓ . All these equations are tested by numerical calculations. However, there are still some aspects to be improved.

- First, We have not found self-consistent EQCs for all parameters for the bare equation in section 4 without Langer's modification from the corresponding Stokes graphs, which actually motivated us to consider the Stark problem at the beginning. We expect to achieve this to a large extent due to the fact that this method is exact if all-orders quantum corrections are included, and TBA equations are applicable in this prescription. The failure might come from the non-matching of wave functions at the semi-classical level, which shows the essence of Langer's modification in the WKB method.
- Second, it seems not easy to directly get the explicit formula for energy frequency from our EQCs to compare with other perturbative formulas. We are also expecting to find a compact form of the TBA equations after wall-crossing as in the case of polynomial potentials. There are some references on this topic like [19, 20] or from the GMN formalism [32], see [41] for example. TBA equation with both ℓ correction and wall-crossing included is also an open question. We would like to consider them in our future work.

Acknowledgements

We would like to thank Keita Imaizumi for his valuable discussions at the early stage. We also thank Hongfei Shu for his kind correspondence. The work of J.Y. is partly supported by the Advanced Research Center for Quantum Physics and Nanoscience, Tokyo Institute of Technology. The work of K.I. is supported in part by Grant-in-Aid for Scientific Research 21K03570 from Japan Society for the Promotion of Science (JSPS).

References

- [1] J. Stark, Beobachtungen über den Effekt des elektrischen Feldes auf Spektrallinien. I. Quereffekt, Annalen der Physik **348** (1914) 965–982.
- [2] E. Schrödinger, Quantisierung als Eigenwertproblem, Annalen Phys. **385** (1926) 437–490.
- [3] P. S. Epstein, The Stark Effect from the Point of View of Schroedinger’s Quantum Theory, Phys. Rev. **28** (1926) 695–710.
- [4] S. Graffi and V. Grecchi, Resonances in Stark effect and perturbation theory, Communications in Mathematical Physics **62** (1978) 83–96.
- [5] R. J. Damburg and V. V. Kolosov, A hydrogen atom in a uniform electric field, Journal of Physics B: Atomic and Molecular Physics **9** (1976) 3149.
- [6] V. V. Kolosov, Stark effect near the peak of the potential barrier, Journal of Physics B: Atomic and Molecular Physics **16** (1983) 25.
- [7] R. E. Langer, On the Connection Formulas and the Solutions of the Wave Equation, Phys. Rev. **51** (1937) 669–676.

- [8] J. P. Dahl and W. P. Schleich, The JWKB Method in Central-Field Problems. Planar Radial Wave Equation and Resolution of Kramers' Dilemma, The Journal of Physical Chemistry A **108** (2004) 8713–8720.
- [9] T. Koike and H. J. Silverstone, Rereading Langer's influential 1937 JWKB paper: the unnecessary Langer transformation; the two \hbar 's, Journal of Physics A: Mathematical and Theoretical **42** (2009) 495206.
- [10] M. H. Rice and R. H. Good, Stark Effect in Hydrogen, J. Opt. Soc. Am. **52** (1962) 239–246.
- [11] J. D. Bekenstein and J. B. Krieger, Stark Effect in Hydrogenic Atoms: Comparison of Fourth-Order Perturbation Theory with WKB Approximation, Phys. Rev. **188** (1969) 130–139.
- [12] J. A. C. Gallas, H. Walther and E. Werner, WKB solution of the Stark effect in hydrogen, Phys. Rev. A **26** (1982) 1775–1778.
- [13] S. H. Patil, Perturbative approach in the WKB analysis: Application to the Stark effect, Phys. Rev. A **59** (1999) 2684–2690.
- [14] J. Écalle, Les fonctions réurgentes (en trois parties), vol. 1, 2 and 3., Université de Paris-Sud, Département de Mathématique, 1981 (1981) .
- [15] R. Balian, G. Parisi and A. Voros, Quartic oscillator, in Feynman Path Integrals (S. Albeverio, P. Combe, R. Høegh-Krohn, G. Rideau, M. Sirugue-Collin, M. Sirugue et al., eds.), (Berlin, Heidelberg), pp. 337–360, Springer Berlin Heidelberg, 1979.
- [16] A. Voros, The return of the quartic oscillator. the complex WKB method, Annales de l'I.H.P. Physique théorique **39** (1983) 211–338.
- [17] A. Voros, Spectre de l'équation de Schrödinger et méthode BKW, Publications Mathématiques d'Orsay, 1981.

- [18] T. Kawai and Y. Takei, Algebraic analysis of singular perturbation theory, vol. 227. American Mathematical Soc., 2005.
- [19] K. Iwaki and T. Nakanishi, Exact WKB analysis and cluster algebras, J. Phys. A **47** (2014) 474009, [1401.7094 [math.CA]]
- [20] K. Iwaki and T. Nakanishi, Exact WKB analysis and cluster algebras II: Simple poles, orbifold points, and generalized cluster algebras, International Mathematics Research Notices (2016) 4375–4417, [1409.4641 [math.CA]].
- [21] H. J. Silverstone, E. Harrell and C. Grot, High-order perturbation theory of the imaginary part of the resonance eigenvalues of the Stark effect in hydrogen and of the anharmonic oscillator with negative anharmonicity, Phys. Rev. A **24** (1981) 1925–1934.
- [22] H. J. Silverstone, JWKB Connection-Formula Problem Revisited via Borel Summation, Phys. Rev. Lett. **55** (1985) 2523–2526.
- [23] N. Sueishi, S. Kamata, T. Misumi and M. Ünsal, On exact-WKB analysis, resurgent structure, and quantization conditions, JHEP **12** (2020) 114, [2008.00379].
- [24] N. Sueishi, S. Kamata, T. Misumi and M. Ünsal, Exact-WKB, complete resurgent structure, and mixed anomaly in quantum mechanics on S^1 , JHEP **07** (2021) 096, [2103.06586].
- [25] H. Dillinger, E. Delabaere and F. Pham, Résurgence de Voros et périodes des courbes hyperelliptiques, Annales de l’Institut Fourier **43** (1993) 163.
- [26] E. Delabaere and F. Pham, Resurgent methods in semi-classical asymptotics, Annales de l’I.H.P. Physique théorique **71** (1999) 1–94.
- [27] P. Dorey and R. Tateo, Anharmonic oscillators, the thermodynamic Bethe ansatz, and nonlinear integral equations, J. Phys. A **32** (1999) L419–L425, [hep-th/9812211].

- [28] P. Dorey, C. Dunning and R. Tateo, The ODE/IM correspondence, J. Phys. A **40** (2007) R205, [[hep-th/0703066](#)].
- [29] K. Ito, M. Mariño and H. Shu, TBA equations and resurgent Quantum Mechanics, JHEP **01** (2019) 228, [[1811.04812](#)].
- [30] Y. Emery, TBA Equations and Quantization Conditions, JHEP **07** (2021) 171, [[2008.13680](#)].
- [31] K. Ito and H. Shu, TBA equations for the Schrödinger equation with a regular singularity, J. Phys. A **53** (2020) 335201–335201, [[1910.09406](#)].
- [32] D. Gaiotto, G. Moore and A. Neitzke, Wall-crossing, Hitchin systems, and the WKB approximation, Advances in Mathematics **234** (2013), [[0907.3987](#) [[hep-th](#)]]
- [33] F. M. Fernández, Direct calculation of Stark resonances in hydrogen, Phys. Rev. A **54** (1996) 1206–1209.
- [34] P. Dorey and R. Tateo, Excited states by analytic continuation of TBA equations, Nucl. Phys. B **482** (1996) 639–659, [[hep-th/9607167](#)].
- [35] B. Gabai and X. Yin, Exact quantization and analytic continuation, JHEP **03** (2023) 082, [[2109.07516](#)].
- [36] K. Imaizumi, Exact conditions for quasi-normal modes of extremal M5-branes and exact WKB analysis, Nucl. Phys. B **992** (2023) 116221, [[2212.04738](#)].
- [37] K. Imaizumi, Applications of Exact WKB analysis to Spectral problems and $\mathcal{N} = 2$ gauge theories. Ph.D. thesis, Tokyo Institute of Technology, 2023.
- [38] I. S. Gradshteyn and I. M. Ryzhik, Table of integrals, series, and products. Academic press, 2014.

- [39] F. M. Fernández and J. Garcia, Comment on “Stark effect in neutral hydrogen by direct integration of the Hamiltonian in parabolic coordinates”, Phys. Rev. A **91** (2015) 066501.
- [40] J. Yang, Resurgent analysis on one-dimensional quantum mechanical systems, Master’s thesis, Tokyo Institute of Technology, 2022.
- [41] H. Ouyang and H. Shu, TBA-like equations for non-planar scattering amplitude/Wilson lines duality at strong coupling, JHEP **05** (2022) 099, [2202.10700].